



DIGITAL ACCESS TO SCHOLARSHIP AT HARVARD

Sources, distribution, and acidity of sulfate–ammonium aerosol in the Arctic in winter–spring

The Harvard community has made this article openly available.
[Please share](#) how this access benefits you. Your story matters.

Citation	Fisher, J.A., D.J. Jacob, Q. Wang, R. Bahreini, C.C. Carouge, M.J. Cubison, J.E. Dibb, T. Diehl, J.L. Jimenez, E.M. Leibensperger, Z. Lu, M.B.J. Meinders, H.O.T. Pye, P.K. Quinn, S. Sharma, D.G. Streets, A. van Donkelaar, and R.M. Yantosca. 2011. "Sources, distribution, and acidity of sulfate-ammonium aerosol in the Arctic in winter-spring." <i>Atmospheric Environment</i> 45: 7301-7318.
Published Version	doi:10.1016/j.atmosenv.2011.08.030
Accessed	February 16, 2015 2:47:59 PM EST
Citable Link	http://nrs.harvard.edu/urn-3:HUL.InstRepos:12712846
Terms of Use	This article was downloaded from Harvard University's DASH repository, and is made available under the terms and conditions applicable to Open Access Policy Articles, as set forth at http://nrs.harvard.edu/urn-3:HUL.InstRepos:dash.current.terms-of-use#OAP

(Article begins on next page)

1 **Sources, distribution, and acidity of sulfate-ammonium aerosol in**
2 **the Arctic in winter-spring**

3 Jenny A. Fisher^a, Daniel J. Jacob^a, Qiaoqiao Wang^a, Roya Bahreini^{b,c}, Claire C. Carouge^a,
4 Michael J. Cubison^{b,d}, Jack E. Dibb^e, Thomas Diehl^{f,g}, Jose L. Jimenez^{b,d}, Eric M.
5 Leibensperger^a, Marcel B. J. Meinders^h, Havala O. T. Pye^{i,1}, Patricia K. Quinn^j, Sangeeta
6 Sharma^k, Aaron van Donkelaar^l, Robert M. Yantosca^a

7 ^a Department of Earth and Planetary Sciences and School of Engineering and Applied Sciences,
8 Harvard University, Cambridge, Massachusetts, USA

9 ^b Cooperative Institute for Research in Environmental Science, University of Colorado, Boulder,
10 Colorado, USA

11 ^c Chemical Sciences Division, NOAA Earth System Research Laboratory, Boulder, Colorado,
12 USA

13 ^d Department of Chemistry and Biochemistry, University of Colorado, Boulder, Colorado, USA

14 ^e Institute for the Study of Earth, Oceans, and Space and Department of Earth Sciences,
15 University of New Hampshire, Durham, New Hampshire, USA

16 ^f Goddard Earth Science and Technology Center, University of Maryland Baltimore County,
17 Baltimore, Maryland, USA

18 ^g Laboratory for Atmospheres, NASA Goddard Space Flight Center, Greenbelt, Maryland, USA

19 ^h Wageningen Universiteit and Research Centre, Food and Biobased Research, Wageningen,
20 Netherlands

21 ⁱ Department of Chemical Engineering, California Institute of Technology, Pasadena, California,
22 USA

23 ^j NOAA Pacific Marine Environmental Laboratory, Seattle, Washington, USA

24 ^k Climate Research Division, Environment Canada, Downsview, Ontario, Canada

25 ^l Department of Physics and Atmospheric Science, Dalhousie University, Canada

26 ¹ now at: Atmospheric Modeling and Analysis Division, U.S. Environmental Protection Agency,
27 Research Triangle Park, North Carolina, USA

28 **Corresponding author:**

29 Jenny A. Fisher (jafisher@fas.harvard.edu)

30 Pierce Hall 110J, 29 Oxford Street, Cambridge, MA 02138, USA

31 Phone: 617.384.7835 / Fax: 617.495.4551

32 **Abstract**

33 We use GEOS-Chem chemical transport model simulations of sulfate-ammonium aerosol data
34 from the NASA ARCTAS and NOAA ARCPAC aircraft campaigns in April 2008, together with
35 longer-term data from surface sites, to better understand aerosol sources in the Arctic in winter-
36 spring and the implications for aerosol acidity. Arctic pollution is dominated by transport from
37 mid-latitudes, and we test the relevant ammonia and sulfur dioxide emission inventories in the
38 model by comparison with wet deposition flux data over the source continents. We find that a
39 complicated mix of natural and anthropogenic sources with different vertical signatures is
40 responsible for sulfate concentrations in the Arctic. East Asian pollution influence is weak in
41 winter but becomes important in spring through transport in the free troposphere. European
42 influence is important at all altitudes but never dominant. West Asia (non-Arctic Russia and
43 Kazakhstan) is the largest contributor to Arctic sulfate in surface air in winter, reflecting a
44 southward extension of the Arctic front over that region. Ammonium in Arctic spring mostly
45 originates from anthropogenic sources in East Asia and Europe, with added contribution from
46 boreal fires, resulting in a more neutralized aerosol in the free troposphere than at the surface.
47 The ARCTAS and ARCPAC data indicate a median aerosol neutralization fraction
48 $[\text{NH}_4^+]/(2[\text{SO}_4^{2-}]+[\text{NO}_3^-])$ of 0.5 mol mol⁻¹ below 2 km and 0.7 mol mol⁻¹ above. We find that
49 East Asian and European aerosol transported to the Arctic is mostly neutralized, whereas West
50 Asian and North American aerosol is highly acidic. Growth of sulfur emissions in West Asia
51 may be responsible for the observed increase in aerosol acidity at Barrow over the past decade.
52 As global ammonia emissions grow over the next century, increasing aerosol neutralization in
53 the Arctic is expected, potentially accelerating Arctic warming through indirect radiative forcing
54 and feedbacks.

55

56 **Keywords:** Arctic; aerosol acidity; sulfate; ammonium; pollution sources

57 ¹

58 **1. Introduction**

59 Long-range transport of pollution from mid-latitudes is a major source of aerosols to the Arctic,
60 with a winter-spring maximum known as Arctic haze (Rahn, 1981a; Quinn et al., 2009). Sulfate

¹ ARCTAS: Arctic Research of the Composition of the Troposphere from Aircraft and Satellites
ARCPAC: Aerosol, Radiation, and Cloud Processes affecting Arctic Climate

61 is the dominant component of this aerosol (Quinn et al., 2007), and it may range from highly
62 acidic to fully neutralized depending on the availability of ammonia. The extent to which sulfate
63 aerosol is neutralized has implications for aerosol radiative forcing (Martin et al., 2004), ice
64 cloud nucleation (Abbatt et al., 2006; Eastwood et al., 2009; Baustian et al., 2010), and
65 heterogeneous chemistry (Fan and Jacob, 1992; Fickert et al., 1999). Here we use the GEOS-
66 Chem 3-D global chemical transport model (CTM) to interpret observations of sulfate-
67 ammonium aerosol composition and acidity from the NASA ARCTAS (Arctic Research of the
68 Composition of the Troposphere from Aircraft and Satellites) and NOAA ARCPAC (Aerosol,
69 Radiation, and Cloud Processes affecting Arctic Climate) aircraft campaigns conducted in April
70 2008, using also ground-based measurements to place the aircraft data in a broader seasonal
71 context. Our objective is to better understand the sources contributing to sulfate, ammonium, and
72 aerosol acidity through the depth of the Arctic troposphere over the winter-spring season.

73
74 High aerosol concentrations in the Arctic in winter-spring reflect a combination of fast transport
75 from mid-latitudes, reduced vertical mixing, and lack of precipitation (Barrie et al., 1981; Raatz
76 and Shaw, 1984; Iversen and Joranger, 1985; Barrie, 1986; Shaw, 1995; Quinn et al., 2007;
77 Garrett et al., 2010). The resulting aerosol radiative forcing may play a major role in driving
78 climate change in the Arctic (Shindell and Faluvegi, 2009), where recent warming has been
79 especially rapid (Trenberth et al., 2007). Scattering sulfate aerosols reflect incoming solar
80 radiation, generally resulting in atmospheric cooling (Quinn et al., 2008). However, warming
81 may result where the surface albedo is very high (Pueschel and Kinne, 1995) or if the sulfate is
82 internally mixed with absorbing aerosol (Jacobson, 2001b). Hygroscopic growth of particles
83 leads to absorption of terrestrial radiation, inducing a direct warming effect that can be
84 particularly efficient during polar night (Ritter et al., 2005). Indirect effects of aerosols on cloud
85 properties typically cause surface cooling (Quinn et al., 2008) but can also warm the surface
86 through interactions with terrestrial radiation (Garrett and Zhao, 2006; Lubin and Vogelmann,
87 2006). The warming is expected to dominate during Arctic winter (Lubin and Vogelmann, 2007).

88
89 The chemical composition of the Arctic aerosol, in particular the extent to which sulfate aerosol
90 is neutralized, has major implications for aerosol radiative forcing. Observations show that
91 ammonia (NH_3) is the main neutralizing agent. It is quantitatively absorbed by the acidic sulfate

92 aerosol, titrating its acidity, reducing its hygroscopicity, and producing solid ammonium sulfate
93 at low relative humidity. The resulting decrease in aerosol water content both reduces the direct
94 radiative forcing of sulfate (Boucher and Anderson, 1995; Adams et al., 2001; Jacobson, 2001a;
95 Martin et al., 2004; J. Wang et al., 2008b) and inhibits homogenous ice nucleation by liquid
96 sulfate-containing particles (Koop et al., 2000). Solid ammonium sulfate particles can also play a
97 role in cold cloud formation by serving as heterogeneous ice nuclei (Abbatt et al., 2006; Wise et
98 al., 2009; Baustian et al., 2010). Hydrophobic dust particles coated with ammonium sulfate are
99 efficient ice nuclei, whereas particles coated with pure sulfuric acid are not (Eastwood et al.,
100 2009). Sulfate aerosol neutralization also suppresses acid-catalyzed heterogeneous bromine
101 reactions thought to be critical in driving ozone and mercury depletion events in Arctic spring
102 (Fan and Jacob, 1992; Ayers et al., 1999; Fickert et al., 1999; Piot and von Glasow, 2008).

103
104 Most of the information on sulfate aerosol in the Arctic has come from surface sites. Early
105 studies attributed sulfate in the North American Arctic to sulfur dioxide (SO₂) sources in Europe
106 and the Soviet Union based on metal tracers (Rahn, 1981b; Raatz and Shaw, 1984; Lowenthal
107 and Rahn, 1985). More recently, Quinn et al. (2009) used the same methodology with data from
108 Barrow, Alaska to show that despite large decreases in emissions and a decreasing trend in
109 sulfate concentrations, the attribution of sulfate sources has not changed over the past 30 years.
110 In contrast, data from Alert, Canada suggest a growing relative contribution from North America
111 as the influence from Eurasian sources has decreased (Gong et al., 2010; Hirdman et al., 2010a).
112 Eurasian emissions are still thought to dominate sulfate concentrations at both Barrow and Alert
113 (Hirdman et al., 2010a; Hirdman et al., 2010b).

114
115 Because the highly stable Arctic boundary layer is decoupled from the free troposphere in
116 winter-spring, measurements at the surface are not representative of the tropospheric column.
117 The sources of sulfate in the Arctic free troposphere are not as well understood as the sources at
118 the surface, and source contributions may vary greatly with altitude (Shindell et al., 2008). Back-
119 trajectory analyses of 1983-1992 aircraft data from the Arctic Gas and Aerosol Sampling
120 Program (AGASP) implied dominant sulfate sources in both the boundary layer and the free
121 troposphere from Europe and the former Soviet Union (Sheridan and Musselman, 1985; Herbert
122 et al., 1989; Parungo et al., 1993). More recent aircraft measurements and model analyses from

123 the Tropospheric Ozone Production about the Spring Equinox (TOPSE) campaign in February-
124 May 2000 suggested dominant sulfate sources from Europe in the boundary layer and from
125 North America in the mid-troposphere (Klonecki et al., 2003; Scheuer et al., 2003).

126
127 A number of CTM studies have investigated the sources of sulfate in the Arctic, with varying
128 results. Simulations for the late 1980s and early 1990s showed a major contribution to Arctic
129 sulfate from the Norilsk industrial site in Siberia. Christensen (1997) found Norilsk to be
130 responsible for 30% of low-altitude sulfate in the Arctic in all seasons, with the remainder from
131 western Europe and Russia. At higher altitudes, Russian and European sources were found to
132 dominate (Christensen, 1997; Tarrasón and Iversen, 1998). More recent work has recognized the
133 growing importance of East Asian emissions, especially in the free troposphere (Koch and
134 Hansen, 2005; Shindell et al., 2008; Huang et al., 2010). While most models agree that Arctic
135 sulfate can be attributed to a mix of anthropogenic sources from Europe, Russia, North America,
136 and East Asia, they disagree considerably both on the relative importance of these sources and on
137 the absolute concentrations of sulfate in the Arctic atmosphere. A recent multi-model sulfate
138 intercomparison by Shindell et al. (2008) showed concentrations varying between models by a
139 factor of 1000 in the Arctic free troposphere, with none of the models able to successfully
140 reproduce observed surface sulfate concentrations or seasonality.

141
142 Little attention has been paid so far to the factors determining the neutralization of acidic sulfate
143 aerosol by ammonia in the Arctic. Combined observations of aerosol sulfate and ammonium,
144 providing a diagnostic of sulfate neutralization, are available from a few Arctic surface sites.
145 Ammonium concentrations also peak in winter-spring but the seasonal amplitude is less than for
146 sulfate, resulting in peak aerosol acidity in winter (Toom-Sauntry and Barrie, 2002). While
147 northern hemispheric NH₃ emissions are estimated to have increased by 20% over the last decade
148 due to agricultural activity (Galloway et al., 2008; Clarisse et al., 2009), data from Barrow show
149 decreasing Arctic ammonium concentrations over the last decade (Quinn et al., 2009).
150 Concurrent decreases in sulfate are proceeding more slowly, resulting in increasing aerosol
151 acidity at Barrow (Quinn et al., 2009). Data at Alert also show a decline in ammonium, but
152 proceeding less rapidly than for sulfate, leading to more neutralized aerosol (Hole et al., 2009).

153 The differences between Barrow and Alert point to different source influences affecting different
154 regions of the Arctic in a time-dependent way.

155
156 Data from the April 2008 ARCTAS and ARCPAC aircraft campaigns based in Fairbanks, Alaska
157 (Brock et al., 2010; Jacob et al., 2010) provide unprecedented information on the vertical
158 distribution of sulfate-ammonium aerosols through the depth of the troposphere in the North
159 American Arctic. Both aircraft included extensive chemical payloads. We use here the GEOS-
160 Chem CTM in combination with the aircraft data and seasonal observations from surface sites to
161 probe the sources of sulfate-ammonium aerosols in the Arctic in winter-spring and the
162 implications for aerosol acidity. Other studies have applied GEOS-Chem to interpretation of
163 ARCTAS/ARCPAC observations of CO (Fisher et al., 2010), carbonaceous aerosols (Q. Wang et
164 al., 2011), HO_x radicals (Mao et al., 2010), and mercury (Holmes et al., 2010).

165

166 **2. GEOS-Chem Simulation**

167 We use the GEOS-Chem CTM version 8-02-03 (<http://geos-chem.org>) to simulate coupled
168 aerosol-oxidant chemistry on the global scale. The model is driven by GEOS-5 assimilated
169 meteorological data from the NASA Goddard Earth Observing System (GEOS) with 6-hour
170 temporal resolution, 47 vertical levels, and 0.5°x0.667° horizontal resolution, regridded to
171 2°x2.5° for input to GEOS-Chem. We initialize the model with a one-year spin-up followed by
172 simulation of January-May 2008.

173

174 The GEOS-Chem coupled aerosol-oxidant simulation was originally described by Park et al.
175 (2004), but the present version includes a number of updates. NH₃ and SO₂ emissions for the
176 simulation period are compiled in Table 1 and shown in Fig. 1. Direct emission of anthropogenic
177 sulfate is included as a small fraction of anthropogenic SO₂ (Chin et al., 2000) and is not
178 included in Table 1. Open biomass burning emissions are from the Fire Location and Monitoring
179 of Burning Emissions (FLAMBE) inventory (Reid et al., 2009), injected into the local planetary
180 boundary layer, with SO₂ and NH₃ emissions scaled to carbon emissions using emission factors
181 from Andreae and Merlet (2001). Unusually large Russian wildfires affected the North American
182 Arctic during ARCTAS/ARCPAC (Warneke et al., 2009). Fisher et al. (2010) found that the
183 FLAMBE emissions for CO needed to be reduced by 47% for Russia and 55% for Southeast

184 Asia to match the aircraft observations and we apply the same corrections here for SO₂ and NH₃.
185 We also include SO₂ emission from both eruptive and non-eruptive (continuous degassing)
186 volcanism. In winter-spring 2008, sustained eruptive activity was recorded at Karymsky and
187 Shiveluch in Kamchatka and Cleveland in the Aleutian Islands. Non-eruptive activity was
188 common throughout our simulation period at a number of volcanoes in Iceland, Kamchatka, and
189 the Aleutian Islands.

190
191 Emitted SO₂ is oxidized to sulfate by the hydroxyl radical (OH) in the gas phase and by ozone
192 (O₃) and hydrogen peroxide (H₂O₂) in the aqueous phase at temperatures above 258 K. Unlike in
193 previous versions of the model (Park et al., 2004; Alexander et al., 2009), cloud volume fraction
194 (used to determine where aqueous SO₂ chemistry occurs) and cloud liquid water content (used to
195 compute the aqueous SO₂ chemistry reaction rates) are now taken directly from the GEOS-5
196 assimilated meteorological fields for each gridbox. Ammonia and nitric acid are partitioned
197 between the gas and the sulfate-nitrate-ammonium aerosol phases using the ISORROPIA II
198 thermodynamic equilibrium model (Fountoukis and Nenes, 2007). Nitrate was usually negligible
199 compared to sulfate in ARCTAS/ARCPAC, both in the observations and the model, owing to the
200 general acidic nature of the aerosol. We discuss the nitrate data briefly in Section 6.

201
202 Aerosol is removed by dry and wet deposition. Dry deposition in GEOS-Chem follows a
203 resistance-in-series scheme (Wesely, 1989) originally described by Y. Wang et al. (1998). Over
204 snow and ice surfaces, we impose an aerosol dry deposition velocity of 0.03 cm s⁻¹ based on
205 eddy-covariance flux measurements by Nilsson and Rannik (2001) and consistent with earlier
206 estimates (Ibrahim et al., 1983; Duan et al., 1988). Wet deposition in the model is based on the
207 scheme described by Liu et al. (2001) with improved representation of scavenging by ice clouds
208 and snow as described by Q. Wang et al. (2011). We assume 100% sulfate and ammonium
209 incorporation into liquid cloud droplets and rime ice for warm and mixed-phase clouds ($T > 258$
210 K) and no incorporation into ice crystals for cold clouds ($T < 258$ K). We also use a higher below-
211 cloud scavenging efficiency for snow than for rain (Murakami et al., 1983). Gaseous NH₃ in the
212 model is efficiently scavenged by liquid precipitation but has a retention efficiency of only 0.05
213 upon riming (which drives precipitation in mixed-phase clouds) and is not scavenged at all in
214 cold clouds (J. Wang et al., 2008a). A sensitivity study assuming complete scavenging of

215 gaseous NH₃ in cold and mixed-phase clouds showed no significant difference in the Arctic
216 relative to the standard simulation because most of the total NH_X (\equiv NH₃+ NH₄⁺) in the Arctic is
217 present as ammonium.

218

219 **3. Testing emission inventories with wet deposition flux data**

220 SO₂ and NH₃ emissions in North America, Europe, and East Asia are potential major sources of
221 sulfate and ammonium aerosol to the Arctic. The corresponding emission inventories used in the
222 model can be tested by comparison with wet deposition flux data over these source continents.
223 Because most of what is emitted is deposited near the source, wet deposition data provide a
224 better constraint on emission than concentration data. While there are large uncertainties
225 associated with modeled precipitation (Dentener et al., 2006; Stephens et al., 2010), we expect
226 the effect of precipitation errors to be small since we consider monthly mean flux data and
227 continental-scale statistics. We used for this analysis data from the ensemble of sites of the U.S.
228 National Atmospheric Deposition Program (NADP; National Atmospheric Deposition Program,
229 2010), the Cooperative Programme for Monitoring and Evaluation of the Long-range
230 Transmission of Air Pollutants in Europe (EMEP; EMEP/CCC, 2010), and the Acid Deposition
231 Monitoring Network in East Asia (EANET; <http://www.eanet.cc/product/index.html>). The
232 EANET network includes a large number of sites labeled as urban, and these were excluded from
233 the comparison as potentially non-representative.

234

235 Figure 2 compares distributions of observed and modeled sulfate and ammonium wet deposition
236 fluxes in April 2008, along with correlation coefficients (r) and normalized mean biases (NMB =
237 $100\% \times \left[\frac{\sum_i (M_i - O_i)}{\sum_i O_i} \right]$, where M_i and O_i are the modeled and observed values,
238 respectively, and the summation is over all sites). The GEOS-Chem sulfate simulation shows
239 good agreement with deposition observations over the U.S. ($r = 0.72$, NMB = +4.7%), consistent
240 with prior model evaluations for this region (Park et al., 2004; Liao et al., 2007; Pye et al., 2009;
241 Drury et al., 2010). Ammonium deposition over the U.S. shows good agreement with NADP
242 observations at low values but a low bias for deposition greater than 0.5 kg NH₄⁺ ha⁻¹ ($r = 0.73$,
243 NMB = -40%). As seen in Fig. 2b, this bias is driven by the agricultural upper Midwest where
244 spring emissions are apparently underestimated. Because transport from North America to the
245 Arctic in spring is mostly from warm conveyor belts over the U.S. east coast (Stohl, 2006; Fisher

246 et al., 2010), we expect errors over the upper Midwest to have limited impact on our Arctic
247 simulation. Over Europe, the model-observation agreement is best at low sulfate values, with
248 model underestimates of high sulfate concentrations observed at a few sites ($r = 0.69$, NMB = -
249 14%). Simulated ammonium deposition over Europe agrees well with observations ($r = 0.61$,
250 NMB = +1.0%). Wet deposition over East Asia is on average too low in GEOS-Chem for both
251 sulfate ($r = 0.85$, NMB = -40%) and ammonium ($r = 0.60$, NMB = -20%). This bias is driven by
252 a few sites with extremely high deposition values (2-3 kg NH₄⁺ ha⁻¹, 4-17 kg SO₄²⁻ ha⁻¹),
253 highlighted in white trim in Fig. 2. When these sites are removed from the comparisons the NMB
254 improves to -0.98% ($r = 0.71$) for sulfate and -6.3% ($r = 0.42$) for ammonium. Overall, our SO₂
255 and NH₃ emission inventories appear unbiased except for the NH₃ underestimate in the upper
256 Midwest U.S.

257

258 In Table 2 we diagnose the acidity of emissions originating from each region as the NH₃/SO₂
259 emission ratio and the NH₄⁺/SO₄²⁻ wet deposition flux ratio. Some difference between these two
260 measures of acidity is expected because of differences in dry deposition, wet scavenging
261 efficiencies, and source locations for SO₂ and NH₃. We do not include NO_x emissions and nitrate
262 wet deposition in this analysis since nitrate does not contribute to aerosol acidity. Unlike sulfate,
263 which can exist in the aerosol phase as sulfuric acid or bisulfate, nitrate only partitions to the
264 aerosol phase in the presence of sufficient ammonia to produce neutralized NH₄NO₃ with no free
265 H⁺ ions. The model emission ratios in Table 2 indicate that emissions in the U.S. lead to highly
266 acidic aerosol, whereas they promote fully neutralized aerosol in Europe and East Asia, at least
267 on the continental scale. While SO₂ emissions in our inventory are similar in Europe and the
268 U.S., NH₃ emissions are much lower in the U.S. (Table 1), consistent with recent estimates (Reis
269 et al., 2009). This difference reflects higher emissions associated with livestock housing, storage,
270 and grazing in Europe (Beusen et al., 2008).

271

272 The differences in emission ratios are reflected in the simulated and observed molar NH₄⁺/SO₄²⁻
273 wet deposition ratios for Europe and the U.S. (Table 2). Over East Asia, wet deposition at
274 EANET sites appears moderately acidic in both the observations ($[\text{NH}_4^+]/2[\text{SO}_4^{2-}] = 0.76$) and
275 the model ($[\text{NH}_4^+]/2[\text{SO}_4^{2-}] = 0.87$), whereas the continental emissions suggest full
276 neutralization. The EANET sites are not, however, representative of the East Asian region as a

277 whole, in large part because there are no observational sites over agricultural regions in India
278 where the NH_3/SO_2 emission ratio is particularly high (Figure 1). GEOS-Chem deposition fluxes
279 averaged over the whole region show aerosol deposition to be as neutralized as expected from
280 the emissions. The $\text{NH}_4^+/\text{SO}_4^{2-}$ ratios indicate more acidic deposition over North America
281 ($[\text{NH}_4^+]/2[\text{SO}_4^{2-}] = 0.76$) than over Europe ($[\text{NH}_4^+]/2[\text{SO}_4^{2-}] = 1.4$). Observed pH shows less
282 regional variation, with average deposition only marginally more acidic over the U.S. (pH =
283 4.93) than over Europe (pH = 5.02). This is due to higher wet deposition fluxes of nitrate (from
284 both aerosol nitrate and gas-phase nitric acid) over Europe. The wet deposition data also indicate
285 partial neutralization by alkaline dust over all three continents. Aircraft observations from
286 ARCPAC indicate that dust particles in the Arctic are generally externally mixed with sulfate,
287 with sulfate mostly in the fine mode ($<0.7 \mu\text{m}$) and dust mostly in the coarse mode (Brock et al.,
288 2010). Further, observations of Asian outflow from the INTEX-B aircraft campaign show the
289 dominant sulfate counterion to be ammonium, not dust (McNaughton et al., 2009; Fairlie et al.,
290 2010). We thus expect that mid-latitude dust would not neutralize the acidity of the submicron
291 sulfate aerosol in the Arctic.

292

293 **4. Simulation and source attribution of Arctic sulfate**

294 **4.1 Aircraft data**

295 The NASA ARCTAS campaign (1-19 April 2008) is described in detail by Jacob et al. (2010).
296 We use here data collected onboard the DC-8 aircraft that was based in Fairbanks, Alaska and
297 covered a large swath of the North American Arctic over 74 flight hours. All concentrations are
298 used at STP conditions (1 atm, 273 K). Speciated aerosol composition data were obtained with
299 an Aerosol Mass Spectrometer (AMS) (Dunlea et al., 2009) measuring submicron aerosol mass
300 and with the SAGA instrumentation package (Dibb et al., 2003) measuring fine aerosol sulfate
301 ($<2.7 \mu\text{m}$) using a mist chamber/ion chromatograph (MC/IC) and bulk sulfate, ammonium,
302 nitrate, calcium, and sodium using filters analyzed by ion chromatography. Speciated aerosol
303 data were also collected during the NOAA ARCPAC campaign (3-23 April 2008) using an AMS
304 onboard the WP-3D aircraft also based in Fairbanks, Alaska (Brock et al., 2010). Flight tracks
305 for ARCTAS and ARCPAC are shown in Fig. 3. The ARCPAC flights covered much less area
306 than ARCTAS, spent more time in the boundary layer, and frequently encountered plumes.

307

308 For comparison to the aircraft data, the GEOS-Chem simulation is sampled along the flight track
309 at the times and locations of the aircraft observations, averaging over either the instrument
310 sampling time or the three-dimensional model grid and time step (Section 2), whichever is
311 coarser. Observations outside the Arctic region (south of 60°N) and those from the stratosphere
312 (diagnosed as $[O_3]/[CO] > 1.25 \text{ mol mol}^{-1}$; Hudman et al., 2008) are excluded. Data from the first
313 two ARCTAS flights (1 and 4 April 2008) are also excluded due to apparent problems with the
314 AMS instrument. Fine-structure plumes are not well simulated by Eulerian CTMs due to
315 numerical diffusion and displacement (Rastigejev et al., 2010). We thus exclude strong biomass
316 burning plumes as diagnosed by observed acetonitrile (CH_3CN) in excess of 225 pptv (Heald et
317 al., 2006; Hudman et al., 2007; Hudman et al., 2008), amounting to 3% of the ARCTAS data and
318 10% of the ARCPAC data. We use a high CH_3CN threshold for this purpose in order to avoid
319 removing biomass burning contributions to background aerosol concentrations, which should be
320 captured by the CTM. We also exclude observations likely to be contaminated by local pollution
321 in Alaska, diagnosed as points below 4 km altitude and within 0.5° of Fairbanks or the Prudhoe
322 Bay oil field. This filter excludes 20% of the ARCPAC data and less than 2% of the ARCTAS
323 data. Finally, we remove one major outlier from each campaign with sulfate in excess of 60 nmol
324 m^{-3} STP. These two outliers represent singularly large concentrations for which we have no
325 explanation.

326
327 Sulfate in the observations includes a contribution from primary sea salt sulfate ($ssSO_4^{2-}$) that is
328 not included in GEOS-Chem. We subtract this contribution from the SAGA filter observations
329 by using a sea salt $[ssSO_4^{2-}]/[Na^+]$ mass ratio of 0.252 (Calhoun et al., 1991). Primary sea salt
330 sulfate estimated in this way accounts for only a small fraction of total bulk sulfate ($1.5 \pm 2.9\%$ on
331 average) and peaks in the boundary layer ($2.6 \pm 3.7\%$ on average below 2 km). No sodium data
332 are available from the AMS measurements, but we assume the sea salt contribution to be
333 negligible. This assumption is reasonable because sodium sulfate does not volatilize rapidly at
334 the temperatures used by the AMS instrument and because these data are only for submicron
335 aerosol while sea salt aerosol is mostly supermicron.

336
337 We compared the three ARCTAS sulfate datasets using reduced major axis regression (Hirsch
338 and Gilroy, 1984). Submicron sulfate measured by the SAGA MC/IC and by the AMS show

339 good agreement ($r = 0.88$, slope = 1.0). SAGA bulk sulfate from the filters generally agrees well
340 with the submicron measurements (AMS: $r = 0.80$, slope = 1.1; SAGA MC/IC: $r = 0.77$, slope =
341 1.1), except during flights on 5 and 8 April 2008 when bulk sulfate concentrations from the
342 SAGA filters were two to three times higher than measured by the other instruments (AMS:
343 slope = 2.1; SAGA MC/IC: slope = 2.8). A large contribution from supermicron sulfate aerosol
344 may arise from sulfate uptake on dust particles (Dibb et al., 2003); however, the data from those
345 two flights were not correlated with dust tracers. We therefore exclude sulfate observations from
346 these two flights from comparisons with GEOS-Chem. For all subsequent ARCTAS analysis, we
347 use the SAGA filter observations due to the similar information content of the SAGA and AMS
348 data.

349
350 Figure 4a shows scatterplots of modeled versus observed sulfate for ARCTAS and ARCPAC.
351 The model has some success in reproducing the variability in the ARCTAS data ($r = 0.60$), with
352 a mean model overestimate of +5.6% and model underestimates at high sulfate concentrations.
353 Model representation of variability is much poorer for ARCPAC ($r = 0.28$), although the mean
354 bias is again small (-5.4%). The small cluster of model points with values in excess of 30 nmol
355 m⁻³ STP reflects a misplaced volcanic plume; without these points the correlation coefficient
356 increases to $r = 0.47$. We conducted model sensitivity simulations to try to understand the poor
357 simulation of variability in ARCPAC but could not relate it to a specific source or conditions,
358 and could not find corrections that would not compromise the simulation of ARCTAS or surface
359 data. The observations do not appear biased as there was internal consistency between the
360 physical, optical and chemical measurements made during ARCPAC (Brock et al., 2010). Our
361 best explanation is that the small sampling domain and time spent in plumes during ARCPAC
362 makes model simulation of the observed variability difficult. The ARCTAS data cover a much
363 larger domain and we view them as more representative.

364
365 Figure 5a shows the mean vertical distributions of observed and modeled sulfate concentrations
366 along the aircraft flight tracks. Model values are decomposed into the contributions from
367 individual sources and regions, as diagnosed by a series of sensitivity simulations with individual
368 sources shut off either globally (ships, biomass burning, natural sources) or for each region
369 shown in Fig. 3 (anthropogenic sources). There is some nonlinearity associated with titration of

370 H₂O₂ in clouds (Chin and Jacob, 1996), the effects of which are included in the relatively small
371 “other” term. We find that there is little mean vertical gradient of sulfate concentrations in either
372 the observations or the model, and that a diversity of sources contribute to sulfate burdens in the
373 North American Arctic at all altitudes. Individual source contributions in the model show much
374 more vertical structure than total sulfate. Below 2 km we find that East Asian, European, and
375 North American anthropogenic sources have comparable influences, each contributing 10-20%
376 of modeled sulfate. The North American influence is limited to the lower troposphere, while
377 European and East Asian contributions are substantial throughout the column. Above 2 km, East
378 Asian emissions are dominant, although still accounting for less than half of the mean total
379 sulfate burden. Natural sources also make substantial contributions to total sulfate. Volcanic
380 sources account for 12-24% of the modeled sulfate at all altitudes, with peak contribution in the
381 mid-troposphere. Dimethyl sulfide (DMS) oxidation is a major source in the lower troposphere,
382 responsible for up to 25% of sulfate below 2 km in the aircraft flight domain during ARCTAS
383 and ARCPAC. We find little contribution ($\leq 2\%$) from open burning to sulfate along the aircraft
384 flight tracks. Recent analyses show sulfate enhancements of up to 30% in biomass burning
385 plumes encountered during both ARCPAC (Warneke et al., 2010) and ARCTAS (Kondo et al.,
386 2011), suggesting that SO₂ emissions from fires in Russia may be larger than assumed in current
387 inventories. Even with increased fire emissions, however, the global SO₂ source would still be
388 dominated by anthropogenic emissions, and the impact of burning on Arctic sulfate would be
389 small. Furthermore, because Asian anthropogenic emissions and Russian fire emissions follow
390 similar pathways of uplift and transport (Fisher et al., 2010), mixing of anthropogenic sulfate
391 with biomass burning plumes en route to the Arctic is likely and may explain the high observed
392 sulfate concentrations in these plumes.

393

394 Roughly 10% of the model sulfate along the flight tracks originates from emissions in West Asia
395 and Southern Siberia (hereafter abbreviated as “West Asia” as most of the emissions are in that
396 part of the region, see Fig. 1). The region includes major industrial areas and oil fields in
397 southwestern Russia and Kazakhstan and represents a sizable source of SO₂ that has likely been
398 growing in recent years based on energy and economic indicators (Grammelis et al., 2006; IEA
399 Statistics, 2009). Emissions from this source are subject to rapid and direct transport to the Arctic

400 around the Siberian high pressure system (Raatz and Shaw, 1984), still active in April during the
401 ARCTAS/ARCPAC period (Fuelberg et al., 2010).

402
403 Recent studies have suggested a large influence on Arctic sulfate from smelters at Norilsk and
404 the Kola Peninsula (Yamagata et al., 2009; Hirdman et al., 2010a; Hirdman et al., 2010b) on the
405 basis of backward trajectories and Lagrangian particle dispersion simulations. In our simulation,
406 these sources (included in our European Arctic region) provide negligible contributions at all
407 altitudes to observed sulfate over the North American Arctic. Indeed, they contribute less than
408 10% to mean concentrations over the High Arctic ($>75^{\circ}\text{N}$), even in surface air in winter. Our
409 finding agrees with analyses from the 1980s showing on the basis of trace element signatures
410 that the Norilsk source had no discernible impact on sulfate at Barrow (Rahn et al., 1983). Since
411 that time, emissions from Norilsk have shown only modest growth, and those from the Kola
412 peninsula have decreased (Boyd et al., 2009; Prank et al., 2010). More recent evidence of limited
413 impact from northern Russian sources comes from a statistical analysis of Arctic snow samples
414 by Hegg et al. (2010) showing that a pollution source associated with high metal loadings
415 characteristic of smelters was responsible for less than 20% of observed sulfur.

416

417 **4.2 Surface data**

418 Surface aerosol data provide a seasonal context for the ARCTAS and ARCPAC results. Figure
419 6a shows monthly mean January-May sulfate concentrations at four surface sites: Alert,
420 Zeppelin, Barrow, and Denali (locations shown in Fig. 3). Observations for both 2008 (thin line)
421 and the 2004-2008 five-year mean (thick line) are shown; the 2008 data are generally
422 representative of the five-year record. Other Alaskan sites from the IMPROVE network (Malm
423 et al., 1994) are not shown as they are located near Denali and have similar concentrations.
424 Sampling frequency varies by site. At Alert and Zeppelin, sampling is continuous with filters
425 changed daily (Zeppelin) or weekly (Alert). At Denali, 24-hr filter samples are collected every
426 three days. Sampling times at Barrow vary by time of year, with 24-hr samples in winter when
427 aerosol concentrations are highest. The Barrow data are subject to large data gaps due to both
428 occasional equipment malfunction and sector-controlled sampling that prevents collection of
429 aerosol contaminated by sources in the town of Barrow. These data gaps, often of a week or
430 more, may introduce biases in the monthly means. In 2008, 24-hr filter samples were collected

431 for 6 days in January, 7 in February, 15 in March, 5 in April, and 18 in May. Also shown in Fig.
432 6a are modeled sulfate concentrations at each site, decomposed into contributions from various
433 sources. For comparison to the surface data, GEOS-Chem is sampled in the lowest model level
434 of the grid box containing the site. Modeled monthly means are calculated based on averages
435 over all days in each month (not just days with valid samples).

436

437 We find that the surface data in April 2008 are consistent across sites (except for Barrow) and
438 with the aircraft data, with mean concentrations of 10-14 nmol m⁻³ STP. Relative to the 2004-
439 2008 mean, Barrow was lower than average in April 2008 (in contrast to the other sites), which
440 could reflect either a sampling bias or the influence of sector-controlled sample collection at
441 Barrow. GEOS-Chem has moderate but non-systematic biases relative to April 2008
442 observations at all sites and is close to or within the interannual variability of the April means.
443 Model source attribution in April is similar to that in the low-altitude aircraft data, with large
444 contributions from East Asia, DMS oxidation, and volcanism. Local Arctic sources such as
445 Prudhoe Bay, Norilsk, and the Kola Peninsula are important at Barrow and Zeppelin, but their
446 influence does not extend to other sites or to the aircraft flight domain.

447

448 Observations at the High Arctic sites (Alert, Zeppelin, Barrow) show only weak seasonal
449 variation from winter to spring, whereas Denali is distinctly lower in winter. We find in the
450 model that the West Asian source is a major contributor to winter sulfate burdens at the High
451 Arctic sites (30-45%), in agreement with back trajectories for black carbon at Alert and Barrow
452 showing influence from this region (Sharma et al., 2006). This source is much less important at
453 Denali, which is generally south of the Arctic front (Barrie and Hoff, 1984). Over Eurasia, the
454 Arctic front in winter often extends as far south as 40°N (Barrie and Hoff, 1984; Stohl, 2006),
455 thus encompassing the sources in the West Asian region. Isentropic transport from these sources
456 to other regions within the Arctic front is enhanced by blocking anticyclones associated with the
457 climatological Siberian high pressure system (Raatz and Shaw, 1984; Iversen and Joranger,
458 1985) and by limited precipitation (Barrie, 1986), while mixing across the Arctic front to areas
459 further south is limited. Southward transport toward Denali is further inhibited by the Brooks
460 Range (Quinn et al., 2002).

461

462 We find that West Asian sources are far more important than Arctic sources in contributing to
463 sulfate concentrations at the Arctic sites in winter. This is because the lower latitudes of the West
464 Asian emissions enables the SO₂ emitted there to be oxidized to sulfate even in winter. By
465 contrast, oxidation of SO₂ emitted from Arctic sources (such as Norilsk and Prudhoe Bay) is
466 restricted by darkness and cold clouds, and we find that most of that SO₂ is deposited rather than
467 oxidized within the Arctic. Heterogeneous SO₂ oxidation mechanisms not included in our model
468 could possibly cause a greater influence from Arctic sources (Alexander et al., 2009), although
469 wintertime sulfate would then be overestimated at Zeppelin and Barrow (not at Alert). The
470 “other” component of our source attribution reflects in part the nonlinearity of the SO₂-sulfate
471 system under oxidant-limited conditions, as discussed above, and is largest in winter when
472 oxidant limitation is most severe. This could also cause some underestimate of our Arctic source
473 contribution.

474

475 All four sites in the model indicate a sharp seasonal transition in source influence from winter to
476 spring, even though changes in total sulfate concentrations are relatively small. In April, the
477 impact of West Asian emissions decreases dramatically at the High Arctic sites while the
478 contributions from East Asia, North America, local Arctic sources, volcanism, and DMS
479 oxidation grow. This transition reflects several processes associated with the end of polar night,
480 including the dissipation of the Siberian High (Raatz and Shaw, 1984), the increase in local
481 oxidant levels, the increase in biogenic DMS emissions (Quinn et al., 2007), and the increasing
482 frequency of warm conveyor belt transport of pollution from East Asia to the Arctic (Liu et al.,
483 2003). Without the West Asian source of SO₂, we find in the model that sulfate concentrations in
484 the High Arctic would be much lower in winter than in spring.

485

486 **4.3 Budget for the High Arctic**

487 We used GEOS-Chem to construct a circumpolar budget of sulfate in the High Arctic (75-90°N),
488 as shown in Fig. 7. Mean concentrations in April are up to 40% lower than along the aircraft
489 flight tracks, reflecting both the greater remoteness and the targeting of plumes by the aircraft.
490 Relative contributions from different sources are similar, although the European contribution is
491 somewhat larger in the High Arctic while the North American contribution is smaller. The

492 contribution from sources in the European Arctic (mainly Norilsk and the Kola Peninsula) is also
493 somewhat larger although still very small, especially in the free troposphere.

494
495 In winter, sulfate sources in the High Arctic are more stratified than in spring (Fig. 7), reflecting
496 the lack of vertical mixing. Consistent with our simulation of the surface sites, the low-altitude
497 winter sulfate budget is dominated by West Asian emissions (32%) followed by European
498 emissions (17%). No other source contributes more than 10%. Concentrations in the free
499 troposphere are much lower than in the boundary layer due largely to limited poleward transport
500 from sources south of the Arctic front in winter. In particular, prevailing transport from East Asia
501 in winter is to the south (winter monsoon) rather than to the north (Liu et al., 2003). Above 5 km,
502 the only substantive contributions to Arctic sulfate are from East Asia (31%), volcanism (20%),
503 and DMS oxidation (15%).

504
505 Our sulfate source attribution disagrees in spring with the multi-model intercomparison of
506 Shindell et al. (2008), which examined the relative sensitivity of Arctic sulfate to sources from
507 North America, Europe, East Asia, and Southeast Asia (but did not consider West Asia). Rather
508 than quantify the absolute burdens associated with each source as we have done here, the authors
509 calculated the decrease in Arctic sulfate associated with a 20% decrease in emissions from each
510 source region. While both approaches are valid, the difference in methodology means that our
511 results can be compared qualitatively but not quantitatively. In contrast to our finding of similar
512 contributions to Arctic surface sulfate from Europe and East Asia, their mean contribution from
513 Europe was more than three times that from East Asia (although with a large spread between
514 models; Shindell et al., 2008). This is because our European SO₂ emissions (7 Tg S a⁻¹ for 2005)
515 are much lower than those used in the Shindell et al. (2008) models (8-25 Tg S a⁻¹ for 2001, with
516 a multi-model mean of 18 Tg S a⁻¹). Smith et al. (2010) show a reduction of only 15-20% in
517 European SO₂ emissions from 2000 to 2005, so that cannot explain the difference. Substantially
518 higher European SO₂ emissions in our simulation would cause an overestimate of sulfate wet
519 deposition in Europe (Section 3) larger than the ~30% attributable to differences in wet removal
520 mechanisms between models (Dentener et al., 2006).

521

522 **5. Simulation and source attribution of Arctic ammonium**

523 5.1 Aircraft data

524 Ammonium was measured during ARCTAS by both the AMS and the SAGA filters.
525 Comparison of these two datasets shows a persistent bias. The two are well correlated ($r = 0.91$),
526 but the AMS ammonium is consistently lower than the SAGA ammonium, with a normalized
527 mean difference of -31%. Conversion of gas-phase NH_3 by acidic aerosols on the filters
528 (especially between sampling and analysis) may explain some of the AMS/SAGA discrepancy.
529 We use the SAGA ammonium observations in what follows as they agree better with the
530 concentrations observed during ARCPAC, although some difference might be expected due to
531 location differences between the two aircraft. Using the AMS observations instead of SAGA
532 would decrease observed ARCTAS ammonium concentrations by 30% relative to the values
533 reported here but would not otherwise affect our conclusions. As for sulfate (Section 4.1), the
534 data have been filtered to exclude stratospheric observations, biomass burning plumes, local
535 pollution, and major outliers. For ammonium, outliers (defined by $[\text{NH}_4^+] > 60 \text{ nmol m}^{-3} \text{ STP}$)
536 include three data points during ARCTAS and six during ARCPAC. We attribute model
537 ammonium to individual sources by conducting sensitivity simulations where we shut off NH_3
538 emissions from each source while leaving SO_2 emissions unchanged to prevent nonlinearities
539 associated with sulfate availability.

540
541 Figures 4b and 5b show that GEOS-Chem reproduces both the mean vertical structure and much
542 of the variability of ammonium in the ARCTAS observations ($r = 0.64$, NMB = -4.8%).
543 Simulation of ammonium during ARCPAC indicates substantial model underestimates,
544 especially below 5 km, as previously found for sulfate (Section 4.1), with $r = 0.43$ and NMB = -
545 19%. As for sulfate, we cannot resolve the discrepancy between GEOS-Chem and ARCPAC in a
546 manner consistent with the other data sets, and we view the ARCTAS data as more
547 representative of the North American Arctic.

548
549 Vertical distributions shown in Fig. 5b indicate peak ammonium concentrations in the mid-
550 troposphere and depletion in the boundary layer, with a larger vertical gradient than for sulfate.
551 Because the aerosol, in general, was acidic (Section 6), ammonium can be regarded as
552 representing total ammonia; gaseous ammonia was not measured on the aircraft but should be
553 negligible based on thermodynamics (Seinfeld and Pandis, 2006). In the free troposphere, the

554 source influences for ammonium are less complex than for sulfate, with more than 80% of Arctic
555 ammonium originating from three sources: East Asian anthropogenic, European anthropogenic,
556 and biomass burning. The anthropogenic source is mainly from agriculture. East Asia is the
557 largest source, accounting for 35-45% of modeled ammonium. Biomass burning is responsible
558 for 20-25%, which reflects the unusually intense Russian fire activity in April 2008 (Warneke et
559 al., 2009; Fisher et al., 2010; Warneke et al., 2010). Below 2 km, the North American
560 anthropogenic and the natural contribution become comparable to the East Asian and European
561 influences, similarly to sulfate. The larger gradient between the boundary layer and the free
562 troposphere for ammonium reflects the greater relative contributions of East Asian and biomass
563 burning sources, which are mainly transported to the Arctic in the free troposphere following
564 lifting by warm conveyor belts (Stohl, 2006; Fisher et al., 2010).

565

566 **5.2 Surface data**

567 Ammonium data from surface sites (Fig. 6b) provide seasonal context for the aircraft data as for
568 sulfate. There is a tendency for higher values in spring than winter but interannual variability is
569 large. The model tends to overestimate observations in winter and this appears driven by the
570 natural source. The GEIA natural NH_3 source used in GEOS-Chem, originally described by
571 Bouwman et al. (1997), includes both oceanic and continental (soil and crop decomposition)
572 emissions. The continental source is dominant at mid-latitudes but there is a non-negligible
573 ocean source in the Arctic including in particular wintertime emission from some areas normally
574 covered by sea ice. It appears likely that the GEIA inventory overestimates oceanic NH_3
575 emissions in the Arctic in winter and that this is the cause for the model ammonium
576 overestimates at Barrow and Zeppelin.

577

578 We find in the model that anthropogenic sources in Europe and West Asia each contribute 20-
579 30% of winter ammonium at Arctic surface sites, even though Europe is a much larger source of
580 NH_3 than West Asia (Fig. 1b, Table 1). This is because West Asian air masses are more readily
581 transported to the Arctic around the Siberian High, as discussed previously for sulfate. In
582 addition, a greater fraction of NH_3 emitted from Europe remains as gaseous NH_3 because of the
583 high NH_3/SO_2 emission ratio (Table 2) and is therefore effectively dry deposited (unlike the
584 aerosol ammonium component) during transport to the Arctic.

585

586 The winter-spring transition in ammonium source contributions in the model is similar to that for
587 sulfate. Dissipation of the polar front increases the influence from East Asia and suppresses the
588 influence from West Asia. For ammonium, the transition is amplified by increased springtime
589 agricultural emissions and biomass burning, whereas in the case of sulfate it was amplified by
590 increased oxidant availability and oceanic biological activity.

591

592 **5.3 Budget for the High Arctic**

593 Our model budget for ammonium in the High Arctic in April 2008 (Fig. 7b) shows source
594 contributions consistent with those derived from the aircraft campaigns. East Asian and
595 European anthropogenic emissions contribute similarly at all altitudes, with additional
596 contributions from biomass burning and natural sources. The European influence peaks in the
597 Eurasian sector of the Arctic beyond the flight domain of the ARCTAS and ARCPAC aircraft,
598 explaining the larger contribution from European emissions to ammonium in the High Arctic
599 (25-35%) than during the aircraft campaigns (15-20%). The spatial heterogeneity of the
600 European influence in spring was also seen in simulation of the surface sites (Fig. 6), which
601 showed more European ammonium at Zeppelin (25%) than Barrow (10%). There is less
602 variation in the East Asian influence, which peaks in the free troposphere for both the aircraft
603 campaigns and the High Arctic domain.

604

605 As for sulfate, ammonium is more stratified in winter than spring, with concentrations more than
606 two times higher below 2 km than above. Consistent with simulation of the surface sites, the
607 low-altitude winter ammonium budget reflects dominant contributions from European, West
608 Asian, and natural sources, although the ocean component of the natural source is probably too
609 high as previously discussed. At 2-5 km the ammonium concentrations represent a diverse mix
610 of sources, while above 5 km East Asia is the single most important source.

611

612 **6. Acidity of the Arctic aerosol**

613 **6.1 Aircraft data**

614 The aerosol observed during the April 2008 aircraft campaigns ranged from highly acidic to fully
615 neutralized. Figure 8a shows the observed aerosol acidity as defined by the relationship of

616 $2[\text{SO}_4^{2-}] + [\text{NO}_3^-]$ versus $[\text{NH}_4^+]$ (Zhang et al., 2007a). We define the mean neutralized fraction as
617 $f = [\text{NH}_4^+] / (2[\text{SO}_4^{2-}] + [\text{NO}_3^-])$ with all concentrations in molar units. We include nitrate for anion
618 closure, but observed nitrate concentrations were generally very small relative to sulfate, with
619 median (interquartile) values of 2.0 (1.2-3.3) nmol m^{-3} STP during ARCTAS and 0.9 (0.2-2.7)
620 nmol m^{-3} STP during ARCPAC. Even when sulfate was neutralized ($f > 0.9$), nitrate contributed
621 on average only 15% of the total anion concentration. Thus $f = 1$ implies a $(\text{NH}_4)_2\text{SO}_4$ sulfate
622 aerosol (solid or aqueous), while $f = 0.5$ implies a NH_4HSO_4 sulfate aerosol in the bulk.
623 Observations with $f > 1$ (excess aerosol ammonium) cannot be reconciled with sulfate-nitrate-
624 ammonium aerosol thermodynamics, but are possible due to the neutralization of organic acids
625 with ammonia (e.g., Dinar et al., 2008; Mensah et al., 2011). These data are also within the
626 precision of the ARCPAC AMS measurement ($\pm 35\%$). These values were mainly associated
627 with biomass burning plumes (identified on the basis of acetonitrile concentrations), where
628 sulfate should be fully neutralized because of the large NH_3 source and where the very large
629 organic aerosol concentrations and organic acid aerosol markers could result in some additional
630 uptake of ammonium.

631
632 We see from Figure 8a that the aerosol was most acidic below 2 km, with median neutralized
633 fraction in the observations of $f = 0.53$ for ARCTAS and $f = 0.50$ for ARCPAC. We find no
634 mean vertical gradient in aerosol acidity above 2 km and thus lump those points together in
635 Figure 8. The aerosol above 2 km was still predominantly acidic, with median observed
636 neutralized fractions of $f = 0.69$ for ARCTAS and $f = 0.65$ for ARCPAC. The vertical gradient in
637 acidity is due to large free tropospheric sources of NH_3 from East Asia and biomass burning, as
638 discussed in Section 5. Figure 8b shows that GEOS-Chem provides a good simulation of the
639 aerosol acidity along the flight tracks, although it slightly underestimates the median neutralized
640 fractions both below 2 km (ARCTAS: $f = 0.45$, ARCPAC: $f = 0.40$) and above (ARCTAS: $f =$
641 0.60 , ARCPAC: $f = 0.66$). The underestimates are largest near the surface, consistent with the
642 low-altitude sulfate overestimates and ammonium underestimates seen in April in the aircraft and
643 surface data (Figs. 5, 6).

644
645 We used the GEOS-Chem sensitivity simulations with suppressed SO_2 and NH_3 emissions from
646 individual source regions to interpret the aerosol acidity observed during ARCTAS and

647 ARCPAC. The simulated aerosol neutralization signatures from the four major anthropogenic
648 source regions (East Asia, Europe, West Asia, and North America) are shown in Fig. 9 as scatter
649 plots of the reductions in sulfate and ammonium along the aircraft trajectories that arise from
650 suppressing each source in the model. Aerosol from North America and West Asia is more acidic
651 than aerosol from East Asia and Europe due to lower NH_3/SO_2 emission ratios (Table 2).
652 Averaged over both campaigns, neutralized fractions in the model are $f = 0.99, 0.75, 0.51,$ and
653 0.41 for the aerosol originating from East Asia, Europe, West Asia, and North America,
654 respectively. The aerosol acidity source attribution in the model helps to explain the observed
655 vertical gradient in aerosol acidity in Fig. 8. The East Asian influence peaks above 2 km,
656 supplying neutralized aerosol to the free troposphere, while the highly acidic North American
657 aerosol is largely confined below 2 km (Fig. 5).

658

659 **6.2 Surface data**

660 The high acidity of the low-altitude aerosol observed and modeled during the aircraft campaigns
661 is consistent with observations at surface sites. In April 2008, the observed surface-level aerosol
662 neutralized fractions were $f = 0.36$ at Alert, $f = 0.39$ at Zeppelin, and $f = 0.40$ at Barrow. Modeled
663 neutralized fractions were $f = 0.41$ at Alert, $f = 0.36$ at Zeppelin, and $f = 0.43$ at Barrow. Figure
664 10 indicates little seasonal variation over winter-spring in aerosol neutralization at any of the
665 sites in the five-year mean. Averaged over January-May for 2004-2008, observed aerosol is most
666 acidic at Alert (mean $f = 0.26$) and most neutralized at Barrow (mean $f = 0.49$); however, this
667 spatial gradient was not evident in 2008 when both model and observations indicate similar
668 neutralization at both sites.

669

670 Long-term observations at Barrow and Alert show conflicting trends in aerosol acidity. At
671 Barrow, January-April ammonium decreased more rapidly than sulfate between 1998 and 2008,
672 leading to a decrease in the ammonium-to-sulfate ratio of $6\% \text{ a}^{-1}$ (significance of 0.01) and
673 implying an increasingly acidic aerosol (Quinn et al., 2009). In contrast, at Alert there was no
674 significant trend in ammonium, sulfate, or the ammonium-to-sulfate ratio over this period,
675 implying no change in aerosol neutralization there. Acidic West Asian emissions provide a major
676 source of sulfate to Barrow but are less important at Alert, in part because deposition is higher en
677 route to Alert due to the more direct, surface-level transport (Sharma et al., 2004; Sharma et al.,

678 2006). In both Kazakhstan and Russia, coal production grew by 20-40% and petroleum by 50-
679 80% between 2000 and 2007 (IEA Statistics, 2009; United Nations Statistics Division,
680 <http://unstats.un.org/unsd/industry/>). This growth may mask decreases in SO₂ from Europe and
681 North America, accounting for the slower decrease in sulfate relative to ammonium observed at
682 Barrow.

683

684 **6.3 Pan-Arctic perspective**

685 Figure 11 shows the mean model distributions of aerosol neutralized fraction in surface air and
686 the free troposphere (5 km) for winter (Jan-Feb) and spring (April). Patterns of aerosol acidity in
687 April are consistent between the aircraft flight tracks and the High Arctic in general, with more
688 acidic aerosol at the surface than above. The most acidic air is found in surface air over northern
689 Eurasia where both West Asian sources and Norilsk have a major influence. Over Russia and
690 Scandinavia, there is a strong meridional gradient in aerosol neutralization. This marks the edge
691 of the polar front, which during April 2008 typically extended to at least 60°N and often further
692 south over Eurasia (Fuelberg et al., 2010). Small areas of high acidity are also evident near local
693 sulfate sources at Prudhoe Bay in Alaska and Norilsk in Russia. In the free troposphere, the
694 aerosol is weakly acidic ($f \approx 0.6$) across the High Arctic. More neutralized air is found over
695 eastern Siberia and the Bering Sea, where the contributions from biomass burning and East
696 Asian emissions are largest.

697

698 We find that the free troposphere is much more acidic in winter ($f \approx 0.3$) than spring, and that the
699 vertical gradient in aerosol acidity is reversed. Free tropospheric aerosol concentrations in winter
700 are low, and high acidity arises from the contributions of volcanism and DMS (Fig. 7), with low
701 Arctic emissions of the latter compensated by higher wind speeds and transport from further
702 south. Modeled neutralization in High Arctic surface air in winter is promoted by high oceanic
703 NH₃ emissions in the Arctic basin. This seasonal trend of increasing surface acidity from winter
704 to spring is not seen in the observations (Fig. 10), again suggesting that these oceanic NH₃
705 emissions are too high in the model as previously discussed. The acidity maxima over the
706 northern Atlantic and Pacific in winter reflect high surface wind speeds that drive NH₃ dry
707 deposition over the oceans. Arctic sulfur emissions from Norilsk and Prudhoe Bay, which
708 produced hotspots of aerosol acidity in April, are less manifest in winter because of the slower

709 SO₂ oxidation. The influence from West Asia, on the other hand, is evident in the widespread
710 region of acidity over Eurasia that extends to lower latitudes within the polar front.

711
712 According to the Intergovernmental Panel on Climate Change (IPCC), global SO₂ emissions are
713 expected to decrease over the coming decades while NH₃ emissions are expected to increase
714 (RCP Database, <http://www.iiasa.ac.at/web-apps/tnt/RcpDb/>). Thus the Arctic aerosol should
715 become increasingly neutralized. However, growth in West Asian energy production is projected
716 for at least the next five years (Klotsvog et al., 2009) and could increase the acidity of the surface
717 aerosol over the short-term horizon as observed by Quinn et al. (2009).

718
719 The extent of sulfate neutralization has implications for the properties of Arctic clouds in winter
720 and spring. The formation and stability of mixed-phase Arctic clouds are highly sensitive to ice
721 nuclei concentration (Harrington et al., 1999; Jiang et al., 2000; Harrington and Olsson, 2001).
722 Arctic air masses with elevated sulfate concentrations have been shown to be depleted in ice
723 nuclei relative to clean air in spring (Borys, 1989), which Girard et al. (2005) found to result in
724 larger ice crystal sizes and enhanced ice precipitation followed by tropospheric dehydration. The
725 dehydration reduces absorption of longwave radiation and cools the atmosphere (Blanchet and
726 Girard, 1995; Curry, 1995), further increasing the dehydration rate (Girard et al., 2005). This
727 relationship results in a positive feedback known as the dehydration-greenhouse feedback (DGF)
728 that can cool the Arctic surface by as much as -3°C (Girard and Stefanof, 2007). Neutralization
729 of sulfate by ammonium may decrease the efficacy of this feedback cycle by providing an
730 increased source of ice nuclei. At the temperatures and relative humidities characteristic of the
731 Arctic free troposphere, ammonium sulfate particles are expected to be predominantly in the
732 solid phase, even accounting for metastability hysteresis (J. Wang et al., 2008a). Ammonium
733 sulfate can therefore serve as heterogeneous ice nuclei under conditions unfavorable to
734 homogeneous nucleation on sulfate particles (Abbatt et al., 2006; Wise et al., 2009; Baustian et
735 al., 2010). If NH₃ emissions increase in the future as projected by the IPCC, an increased
736 population of ammonium sulfate particles in the Arctic may lead to increased ice nuclei
737 formation, reduced dehydration, and enhanced Arctic warming.

738
739 **7. Conclusions**

740 We used observations from the ARCTAS and ARCPAC aircraft campaigns in April 2008
741 together with longer-term records from Arctic surface sites to better understand the sources of
742 sulfate-ammonium aerosol in the Arctic in winter-spring and the implications for Arctic aerosol
743 acidity. Aerosol concentrations in the Arctic are particularly high in winter-spring. Sulfate is a
744 dominant component of this aerosol, and its neutralization by ammonium has important
745 implications for climate forcing. Our analysis was based on simulations of observations with the
746 GEOS-Chem chemical transport model, including sensitivity simulations to diagnose the
747 contributions from different source regions and source types to aerosol concentrations and
748 acidity.

749
750 Observed wet deposition fluxes of sulfate and ammonium in the U.S., Europe, and East Asia in
751 April 2008 were used to test the emissions of SO₂ and NH₃ from these continental source regions
752 in GEOS-Chem. Results showed good agreement except for ammonium over the Midwest U.S.,
753 where spring agricultural emissions are apparently underestimated. Using the SO₂/NH₃ emission
754 ratio and the SO₄²⁻/NH₄⁺ wet deposition flux ratio, we found that spring emissions are conducive
755 to full neutralization by large NH₃ inputs from agricultural activity in both Europe ($E_{NH3}/2E_{SO2} =$
756 1.3 mol mol^{-1}) and East Asia ($E_{NH3}/2E_{SO2} = 1.2 \text{ mol mol}^{-1}$), whereas emissions in the U.S. should
757 lead to much more acidic aerosol ($E_{NH3}/2E_{SO2} = 0.3 \text{ mol mol}^{-1}$).

758
759 Sulfate concentrations in the aircraft observations were relatively uniform through the depth of
760 the troposphere, and this is well simulated with the model. The model shows that a diversity of
761 sources contribute to sulfate burdens in spring, with major contributions at all altitudes from East
762 Asian and European anthropogenic sources, oxidation of DMS, and volcanic emission. North
763 American anthropogenic emissions are also important below 2 km. Surface sites north of the
764 Arctic front (Barrow, Alert, Zeppelin) show little variation of total sulfate from winter to spring,
765 consistent with the model, but the model indicates an important seasonal shift in source
766 attribution with non-Arctic West Asian sources (southwest Russia and Kazakhstan) dominating
767 in winter. This strong West Asian influence dissipates in the spring with the northward
768 contraction of the polar front, to be replaced by increasing sulfate contributions from East Asia
769 and DMS emissions. We find that industrial sources of SO₂ in the Arctic (Norilsk, Kola
770 Peninsula, Prudhoe Bay) make little contribution to the Arctic sulfate budget.

771
772 Our finding of non-Arctic West Asia (southwest Russia and Kazakhstan) as a major source
773 region for Arctic sulfate in winter, distinct from the well-known sources in northwest Russia and
774 Siberia, does not seem to have been recognized before. Sharma et al. (2006) show back-
775 trajectories for black carbon at Alert that also point to a significant source from that region. Oil
776 fields and industrial centers in that region are a large and growing source of SO₂. These
777 emissions are released at low enough latitudes to enable oxidation of SO₂ in winter but are still
778 within the boundary of the Arctic front (which over Eurasia can extend as far south as 40°N in
779 winter; Barrie and Hoff, 1984), facilitating rapid low-altitude transport to the Arctic. By contrast,
780 oxidation of SO₂ emitted from Arctic industrial sources is limited in winter by darkness and cold
781 clouds. West Asian emissions are highly uncertain and more work is needed to quantify them in
782 view of their apparent importance as a source of Arctic sulfate.

783
784 Ammonium concentrations observed during ARCTAS and ARCPAC were higher in the free
785 troposphere than in the boundary layer. The source influences in spring are less complex than for
786 sulfate, with 80% of free tropospheric ammonium originating from a mix of biomass burning and
787 East Asian and European anthropogenic emissions. Biomass burning and East Asian influences
788 are stronger in the free troposphere due to lifting in warm conveyor belts over the Pacific.
789 Surface sites show a general tendency for higher ammonium concentrations in spring than winter
790 due to increased NH₃ emission associated with the onset of agricultural fires and fertilizer
791 application. The model overestimates observed winter ammonium and therefore aerosol
792 neutralization at the surface sites, likely because of poor representation of sea ice suppression of
793 oceanic NH₃ emission in the GEIA inventory of Bouwman et al. (1997). Work is needed to better
794 quantify oceanic NH₃ emissions and their seasonal variation.

795
796 The aircraft data indicated predominantly acidic aerosol throughout the depth of the Arctic
797 troposphere in spring, with higher acidity below 2 km (median neutralized fraction $f =$
798 $[\text{NH}_4^+]/(2[\text{SO}_4^{2-}] + [\text{NO}_3^-]) = 0.5$) than above (median $f = 0.7$). Observed acidity at surface sites
799 was even higher ($f = 0.4$). This gradient reflects the preferential transport of neutralized biomass
800 burning and East Asian aerosol in the free troposphere. Simulation with GEOS-Chem indicates
801 that the free troposphere is more acidic in winter than in spring, and natural emissions play a

802 major role in driving this seasonality. DMS oxidation and volcanic emission provide a source of
803 sulfate throughout the troposphere that is not matched by natural NH₃ emission. At the surface,
804 observations show no seasonal variation in aerosol neutralization from winter to spring.

805
806 Source neutralization signatures computed from GEOS-Chem and consistent with observations
807 indicate that East Asia and Europe provide neutralized aerosol to the Arctic, while West Asia is
808 the dominant source of acidic aerosol. Our results help explain observed long-term trends in
809 aerosol acidity at surface sites. Observations from Barrow show increasing acidity over the last
810 decade due to more rapid decreases in ammonium than sulfate (Quinn et al., 2008), while there
811 has been no change in aerosol acidity at Alert. Because Barrow is more heavily influenced by
812 acidic West Asian sources than Alert, the impacts at Barrow of recent decreases in SO₂
813 emissions from North America and Europe may have been masked by concurrent increases in
814 emissions from coal and petroleum production in Russia and Kazakhstan. While further growth
815 in this region is expected over the next few years (Klotsvog et al., 2009), longer-term projections
816 suggest global decreases in SO₂ emissions over the next decades together with increases in NH₃
817 emissions (RCP Database, <http://www.iiasa.ac.at/web-apps/tnt/RcpDb/>). The resultant increase
818 in the concentration of ammonium sulfate aerosols may lead to enhanced ice nuclei formation,
819 initiating a dehydration-greenhouse feedback that could accelerate warming in the Arctic.

820
821 **Acknowledgments.** This work was supported by the NASA Tropospheric Chemistry Program.
822 We thank A. M. Middlebrook for obtaining the ARCPAC AMS data.

823 **References**

- 824 Abbatt, J.P.D., Benz, S., Czizco, D.J., Kanji, Z., Lohmann, U., Möhler, O., 2006. Solid
825 Ammonium Sulfate Aerosols as Ice Nuclei: A Pathway for Cirrus Cloud Formation. *Science*
826 313, 1770-1773.
- 827 Adams, P.J., Seinfeld, J.H., Koch, D., Mickley, L.J., Jacob, D.J., 2001. General circulation
828 model assessment of direct radiative forcing by the sulfate-nitrate-ammonium-water inorganic
829 aerosol system. *Journal of Geophysical Research* 106, 1097-1111.
- 830 Alexander, B., Park, R.J., Jacob, D.J., Gong, S., 2009. Transition metal-catalyzed oxidation of
831 atmospheric sulfur: Global implications for the sulfur budget. *Journal of Geophysical Research*
832 114.
- 833 Andreae, M.O., Merlet, P., 2001. Emission of trace gases and aerosols from biomass burning.
834 *Global Biogeochemical Cycles* 15, 955-966.
- 835 Ayers, G.P., Gillett, R.W., Cainey, J.M., Dick, A.L., 1999. Chloride and bromide loss from sea-
836 salt particles in Southern Ocean air. *Journal of Atmospheric Chemistry* 33, 299-319.
- 837 Barrie, L.A., 1986. Arctic air pollution: An overview of current knowledge. *Atmospheric*
838 *Environment* 20, 643-663.
- 839 Barrie, L.A., Hoff, R.M., 1984. The oxidation rate and residence time of sulphur dioxide in the
840 Arctic atmosphere. *Atmospheric Environment* 18, 2711-2722.
- 841 Barrie, L.A., Hoff, R.M., Daggupati, S.M., 1981. The influence of mid-latitudinal pollution
842 sources on haze in the Canadian Arctic. *Atmospheric Environment* 15, 1407-1419.
- 843 Baughcum, S.L., Tritz, T.G., Henderson, S.C., Pickett, D.C., 1996. Scheduled Civil Aircraft
844 Emission Inventories for 1992: Database Development and Analysis. NASA Contractor Report
845 4700.
- 846 Baustian, K.J., Wise, M.E., Tolbert, M.A., 2010. Depositional ice nucleation on solid ammonium
847 sulfate and glutaric acid particles. *Atmospheric Chemistry and Physics* 10, 2307-2317.
- 848 Beusen, A.H.W., Bouwman, A.F., Heuberger, P.S.C., Van Drecht, G., Van Der Hoek, K.W.,
849 2008. Bottom-up uncertainty estimates of global ammonia emissions from global agricultural
850 production systems. *Atmospheric Environment* 42, 6067-6077.
- 851 Blanchet, J.-P., Girard, E., 1995. Water vapor-temperature feedback in the formation of
852 continental Arctic air: its implication for climate. *Science of the Total Environment* 160/161,
853 793-802.
- 854 Borys, R.D., 1989. Studies of ice nucleation by Arctic aerosol on AGASP-II. *Journal of*
855 *Atmospheric Chemistry* 9, 169-185.

856 Boucher, O., Anderson, T.L., 1995. General circulation model assessment of the sensitivity of
857 direct climate forcing by anthropogenic sulfate aerosols to aerosol size and chemistry. *Journal of*
858 *Geophysical Research* 100, 26117-26134.

859 Bouwman, A.F., Lee, D.S., Asman, W.A.H., Dentener, F.J., Van Der Hoek, K.W., Olivier,
860 J.G.J., 1997. A global high-resolution emission inventory for ammonia. *Global Biogeochemical*
861 *Cycles* 11, 561-587.

862 Boyd, R., Barnes, S.-J., De Caritat, P., Chekushin, V.A., Melezhik, V.A., Reimann, C., Zientek,
863 M.L., 2009. Emissions from the copper–nickel industry on the Kola Peninsula and at Noril'sk,
864 Russia. *Atmos. Environ.* 43, 1474-1480.

865 Brock, C.A., Cozic, A., Bahreini, R., Froyd, K.D., Middlebrook, A.M., McComiskey, A.,
866 Brioude, J., Cooper, O.R., Stohl, A., Aikin, K.C., de Gouw, J.A., Fahey, D.W., Ferrare, R.A.,
867 Gao, R.-S., Gore, W., Holloway, J.S., Hübler, G., Jefferson, A., Lack, D.A., Lance, S.M., Moore,
868 R.H., Murphy, D.M., Nenes, A., Novelli, P.C., Nowak, J.B., Ogren, J.A., Peischl, J., Pierce,
869 R.B., Pilewski, P., Quinn, P.K., Ryerson, T.B., Schmidt, K.S., Schwarz, J.P., Sodemann, H.,
870 Spackman, J.R., Stark, H., Thomson, D.S., Thornberyy, T., Veres, P., Watts, L.A., Warneke, C.,
871 Wollny, A.G., 2010. Characteristics, Sources, and Transport of Aerosols Measured in Spring
872 2008 During the Aerosol, Radiation, and Cloud Processes Affecting Arctic Climate (ARCPAC)
873 Project. *Atmospheric Chemistry and Physics Discussions* 10, 27361-27434.

874 Calhoun, J.A., Bates, T.S., Charlson, R.J., 1991. Sulfur isotope measurements of submicrometer
875 sulfate aerosol particles over the Pacific Ocean. *Geophysical Research Letters* 18.

876 Chin, M., Jacob, D.J., 1996. Anthropogenic and natural contributions to tropospheric sulfate: A
877 global model analysis. *Journal of Geophysical Research* 101, 18691-18699.

878 Chin, M., Rood, R., Lin, S., Müller, J., Thompson, A., 2000. Atmospheric sulfur cycle simulated
879 in the global model GOCART: Model description and global properties. *Journal of Geophysical*
880 *Research* 105, 24671.

881 Christensen, J.H., 1997. The Danish Eulerian Hemispheric Model - a three-dimensional air
882 pollution model used for the Arctic. *Atmospheric Environment* 31, 4169-4191.

883 Clarisse, L., Clerbaux, C., Dentener, F., Hurtmans, D., Coheur, P.-F., 2009. Global ammonia
884 distribution derived from infrared satellite observations. *Nature Geoscience* 2, 479-483.

885 Curry, J.A., 1995. Interactions among aerosols, clouds, and climate of the Arctic Ocean. *Science*
886 *of the Total Environment* 160/161, 777-791.

887 Dentener, F., Drevet, J., Lamarque, J.F., Bey, I., Eickhout, B., Fiore, A.M., Hauglustaine, D.A.,
888 Horowitz, L.W., Krol, M., Kulshrestha, U.C., Lawrence, M., Galy-Lacaux, C., Rast, S., Shindell,
889 D., Stevenson, D., Van Noije, T., Atherton, C., Bell, N., Bergman, D., Butler, T., Cofala, J.,
890 Collins, B., Doherty, R., Ellingsen, K., Galloway, J., Gauss, M., Montanaro, V., Müller, J.F.,
891 Pitari, G., Rodriguez, J., Sanderson, M., Solomon, F., Strahan, S., Schultz, M., Sudo, K., Szopa,
892 S., Wild, O., 2006. Nitrogen and sulfur deposition on regional and global scales: A multimodel
893 evaluation. *Global Biogeochem. Cy.* 20, GB4003.

894 Dibb, J.E., Talbot, R.W., Scheuer, E.M., Seid, G., Avery, M.A., Singh, H.B., 2003. Aerosol
895 chemical composition in Asian continental outflow during the TRACE-P campaign: Comparison
896 with PEM-West B. *Journal of Geophysical Research* 108, 8815.

897 Diehl, T., 2009. A global inventory of volcanic SO₂ emissions for hindcast scenarios,
898 http://www-lscedods.cea.fr/aerocom/AEROCOM_HC/volc/ (Documents updated in subsequent
899 years after 2009). Last accessed on October 2010.

900 Dinar, E., Anttila, T., Rudich, Y., 2008. CCN activity and hygroscopic growth of organic
901 aerosols following reactive uptake of ammonia. *Environmental Science & Technology* 42, 793-
902 799.

903 Drury, E., Jacob, D.J., Spurr, R.J.D., Wang, J., Shinozuka, Y., Anderson, B.E., Clarke, A.D.,
904 Dibb, J.E., McNaughton, C., Weber, R., 2010. Synthesis of satellite (MODIS), aircraft
905 (ICARTT), and surface (IMPROVE, EPA-AQS, AERONET) aerosol observations over eastern
906 North America to improve MODIS aerosol retrievals and constrain surface aerosol
907 concentrations and sources. *Journal of Geophysical Research* 115, D14204.

908 Duan, B., Fairall, C.W., Thomson, D.W., 1988. Eddy correlation measurements of the dry
909 deposition of particles in wintertime. *Journal of Applied Meteorology* 27, 642-652.

910 Dunlea, E.J., DeCarlo, P.F., Aiken, A.C., Kimmel, J.R., Peltier, R.E., Weber, R.J., Tomlinson, J.,
911 Collins, D.R., Shinozuka, Y., McNaughton, C.S., Howell, S.G., Clarke, A.D., Emmons, L.K.,
912 Apel, E.C., Pfister, G.G., van Donkelaar, A., Martin, R.V., Millet, D.B., Heald, C.L., Jimenez,
913 J.L., 2009. Evolution of Asian Aerosols during Transpacific Transport in INTEX-B.
914 *Atmospheric Chemistry and Physics* 9, 7257-7287.

915 Eastwood, M.L., Cremel, S., Wheeler, M., Murray, B.J., Girard, E., Bertram, A.K., 2009. Effects
916 of sulfuric acid and ammonium sulfate coatings on the ice nucleation properties of kaolinite
917 particles. *Geophysical Research Letters* 36, L02811.

918 EMEP/CCC, 2010. Acidifying and eutrophying compounds and particulate matter. EMEP Co-
919 operative Programme for Monitoring and Evaluation of the Long-Range Transmission of Air
920 Pollutants in Europe, Kjeller, Norway.

921 Eyring, V., Köhler, H.W., Lauer, A., Lempert, B., 2005a. Emissions from international shipping:
922 2. Impact of future technologies on scenarios until 2050. *Journal of Geophysical Research* 110,
923 D17306.

924 Eyring, V., Köhler, H.W., van Aardenne, J., Lauer, A., 2005b. Emissions from international
925 shipping: 1. The last 50 years. *Journal of Geophysical Research* 110, D17305.

926 Fairlie, T.D., Jacob, D.J., Dibb, J.E., Alexander, B., Avery, M.A., van Donkelaar, A., Zhang, L.,
927 2010. Impact of mineral dust on nitrate, sulfate, and ozone in transpacific Asian pollution
928 plumes. *Atmos. Chem. Phys.* 10, 3999-4012.

929 Fan, S.-M., Jacob, D.J., 1992. Surface ozone depletion in Arctic spring sustained by bromine
930 reactions on aerosols. *Nature* 359, 522-524.

- 931 Fickert, S., Adams, J.W., Crowley, J.N., 1999. Activation of Br₂ and BrCl via uptake of HOBr
932 onto aqueous salt solutions. *Journal of Geophysical Research* 104, 23719-23727.
- 933 Fisher, J.A., Jacob, D.J., Purdy, M.T., Kopacz, M., Le Sager, P., Carouge, C., Holmes, C.D.,
934 Yantosca, R.M., Batchelor, R.L., Strong, K., Diskin, G.S., Fuelberg, H.E., Holloway, J.S., Hyer,
935 E.J., McMillan, W.W., Warner, J., Streets, D.G., Zhang, Q., Wang, Y., Wu, S., 2010. Source
936 attribution and interannual variability of Arctic pollution in spring constrained by aircraft
937 (ARCTAS, ARCPAC) and satellite (AIRS) observations of carbon monoxide. *Atmospheric*
938 *Chemistry and Physics* 10, 977-996.
- 939 Fountoukis, C., Nenes, A., 2007. ISORROPIA II: a computationally efficient thermodynamic
940 equilibrium model for K⁺-Ca²⁺-Mg²⁺-NH⁺-Na⁺-SO₂-NO-Cl-H₂O aerosols.
941 *Atmospheric Chemistry and Physics* 7, 4639-4659.
- 942 Fuelberg, H.E., Harrigan, D.L., Sessions, W., 2010. A meteorological overview of the ARCTAS
943 2008 mission. *Atmos. Chem. Phys.* 10, 817-842.
- 944 Galloway, J.N., Townsend, A.R., Erisman, J.W., Bekunda, M., Cai, Z., Freney, J.R., Martinelli,
945 L.A., Seitzinger, S.P., Sutton, M.A., 2008. Transformation of the Nitrogen Cycle: Recent Trends,
946 Questions, and Potential Solutions. *Science* 320, 889-892.
- 947 Garrett, T.J., Zhao, C., 2006. Increased Arctic cloud longwave emissivity associated with
948 pollution from mid-latitudes. *Nature* 440, 787-789.
- 949 Garrett, T.J., Zhao, C., Novelli, P.C., 2010. Assessing the relative contributions of transport
950 efficiency and scavenging to seasonal variability in Arctic aerosol. *Tellus* 62B, 190-196.
- 951 Girard, E., Blanchet, J.-P., Dubois, Y., 2005. Effects of arctic sulphuric acid aerosols on
952 wintertime low-level atmospheric ice crystals, humidity and temperature at Alert, Nunavut.
953 *Atmospheric Research* 73, 131-148.
- 954 Girard, E., Stefanof, A., 2007. Assessment of the dehydration-greenhouse feedback over the
955 Arctic during February 1990. *International Journal of Climatology* 27, 1047-1058.
- 956 Gong, S.L., Zhao, T.L., Sharma, S., Toom-Saunty, D., Lavoué, D., Zhang, X.B., Leitch, W.R.,
957 Barrie, L.A., 2010. Identification of trends and interannual variability of sulfate and black carbon
958 in the Canadian High Arctic: 1981-2007. *Journal of Geophysical Research* 115, D07305.
- 959 Grammelis, P., Koukouzas, N., Skodras, G., Kakaras, E., Tumanovsky, A., Kotler, V., 2006.
960 Refurbishment priorities at the Russian coal-fired power sector for cleaner energy production—
961 Case studies. *Energy Policy* 34, 3124-3136.
- 962 Harrington, J.Y., Olsson, P.Q., 2001. On the potential influence of ice nuclei on surface-forced
963 marine stratocumulus cloud dynamics. *Journal of Geophysical Research* 106, 27473-27484.
- 964 Harrington, J.Y., Reisin, T., Cotton, W.R., Kreidenweis, S.M., 1999. Cloud resolving
965 simulations of Arctic stratus Part II: Transition-season clouds. *Atmospheric Research* 51, 45-75.

- 966 Heald, C.L., Jacob, D.J., Turquety, S., Hudman, R.C., Weber, R.J., Sullivan, A.P., Peltier, R.E.,
967 Atlas, E.L., de Gouw, J.A., Warneke, C., Holloway, J.S., Neuman, J.A., Flocke, F.M., Seinfeld,
968 J.H., 2006. Concentrations and sources of organic carbon aerosols in the free troposphere over
969 North America. *J. Geophys. Res.* 111, D23S47.
- 970 Hegg, D.A., Warren, S.G., Grenfell, T.C., Doherty, S.J., Clarke, A.D., 2010. Sources of light-
971 absorbing aerosol in arctic snow and their seasonal variation. *Atmospheric Chemistry and*
972 *Physics* 10, 10923-10938.
- 973 Herbert, G.A., Harris, J.M., Bodhaine, B.A., 1989. Atmospheric transport during the AGASP-II:
974 The Alaskan flights (2-10 April 1986). *Atmospheric Environment* 23, 2521-2535.
- 975 Hirdman, D., Burkhardt, J.F., Sodemann, H., Eckhardt, S., Jefferson, A., Quinn, P.K., Sharma, S.,
976 Ström, J., Stohl, A., 2010a. Long-term trends of black carbon and sulphate aerosol in the Arctic:
977 changes in atmospheric transport and source region emissions. *Atmospheric Chemistry and*
978 *Physics* 10, 9351-9368.
- 979 Hirdman, D., Sodemann, H., Eckhardt, S., Burkhardt, J.F., Jefferson, A., Mefford, T., Quinn, P.K.,
980 Sharma, S., Ström, J., Stohl, A., 2010b. Source identification of short-lived air pollutants in the
981 Arctic using statistical analysis of measurement data and particle dispersion model output.
982 *Atmospheric Chemistry and Physics* 10, 669-693.
- 983 Hirsch, R.M., Gilroy, E.J., 1984. Methods of fitting a straight line to data: examples in water
984 resources. *Journal of the American Water Resources Association* 20, 705-711.
- 985 Hole, L.R., Christensen, J.H., Ruoho-Airola, T., Tørseth, K., Ginzburg, V., Glowacki, P., 2009.
986 Past and future trends in concentrations of sulphur and nitrogen compounds in the Arctic.
987 *Atmospheric Environment* 43, 928-939.
- 988 Holmes, C.D., Jacob, D.J., Corbitt, E.S., Mao, J., Yang, X., Talbot, R., Slemr, F., 2010. Global
989 atmospheric model for mercury including oxidation by bromine atoms. *Atmospheric Chemistry*
990 *and Physics Discussions* 10, 19845-19900.
- 991 Huang, L., Gong, S.L., Jia, C.Q., Lavoué, D., 2010. Relative contributions of anthropogenic
992 emissions to black carbon aerosol in the Arctic. *Journal of Geophysical Research* 115, D19208.
- 993 Hudman, R.C., Jacob, D.J., Turquety, S., Leibensperger, E.M., Murray, L.T., Wu, S., Gilliland,
994 A.B., Avery, M., Bertram, T.H., Brune, W., 2007. Surface and lightning sources of nitrogen
995 oxides over the United States: Magnitudes, chemical evolution, and outflow. *Journal of*
996 *Geophysical Research* 112, D12S05.
- 997 Hudman, R.C., Murray, L.T., Jacob, D.J., Millet, D.B., Turquety, S., Wu, S., Blake, D.R.,
998 Goldstein, A.H., Holloway, J., Sachse, G.W., 2008. Biogenic vs. anthropogenic sources of CO
999 over the United States. *Geophysical Research Letters* 35, L04801
- 1000 Ibrahim, M., Barrie, L.A., Fanaki, F., 1983. An experimental and theoretical investigation of the
1001 dry deposition of particles to snow, pine trees, and artificial collectors. *Atmospheric*
1002 *Environment* 17, 781-788.

- 1003 IEA Statistics, 2009. Energy Statistics of Non-OECD Countries: 2009 Edition. International
1004 Energy Agency.
- 1005 Iversen, T., Joranger, E., 1985. Arctic air pollution and large scale atmospheric flows.
1006 Atmospheric Environment 19, 2099-2108.
- 1007 Jacob, D.J., Crawford, J.H., Maring, H., Clarke, A.D., Dibb, J.E., Emmons, L.K., Ferrare, R.A.,
1008 Hostetler, C.A., Russell, P.B., Singh, H.B., Thompson, A.M., Shaw, G.E., McCauley, E.,
1009 Pederson, J.R., Fisher, J.A., 2010. The Arctic Research of the Composition of the Troposphere
1010 from Aircraft and Satellites (ARCTAS) mission: design, execution, and first results.
1011 Atmospheric Chemistry and Physics 10, 5191-5212.
- 1012 Jacobson, M.Z., 2001a. Global direct radiative forcing due to multicomponent anthropogenic and
1013 natural aerosols. Journal of Geophysical Research 106, 1551-1568.
- 1014 Jacobson, M.Z., 2001b. Strong radiative heating due to the mixing state of black carbon in
1015 atmospheric aerosols. Nature 409, 695-697.
- 1016 Jiang, H., Cotton, W.R., Pinto, J.O., Curry, J.A., Weissbluth, M.J., 2000. Cloud Resolving
1017 Simulations of Mixed-Phase Arctic Stratus Observed during BASE: Sensitivity to Concentration
1018 of Ice Crystals and Large-Scale Heat and Moisture Advection. Journal of the Atmospheric
1019 Sciences 57, 2105-2117.
- 1020 Klonecki, A., Hess, P., Emmons, L., Smith, L., Orlando, J., Blake, D., 2003. Seasonal changes in
1021 the transport of pollutants into the Arctic troposphere-model study. Journal of Geophysical
1022 Research 108, 8367.
- 1023 Klotsvog, F.N., Sukhotin, A.B., Chernova, L.S., 2009. Forecast of Economic Growth in Russia,
1024 Belarus, Kazakhstan, and Ukraine within the Unified Economic Space. Studies on Russian
1025 Economic Development 20, 366-372.
- 1026 Koch, D., Hansen, J., 2005. Distant origins of Arctic black carbon: A Goddard Institute for Space
1027 Studies ModelE experiment. Journal of Geophysical Research 110, D04204.
- 1028 Kondo, Y., Matsui, H., Moteki, N., Sahu, L., Takegawa, N., Kajino, M., Zhao, Y., Cubison, M.J.,
1029 Jimenez, J.L., Vay, S., Diskin, G.S., Anderson, B., Wisthaler, A., Mikoviny, T., Fuelberg, H.E.,
1030 Blake, D.R., Huey, G., Weinheimer, A.J., Knapp, D.J., Brune, W.H., 2011. Emissions of black
1031 carbon, organic, and inorganic aerosols from biomass burning in North America and Asia in
1032 2008 Journal of Geophysical Research in press.
- 1033 Koop, T., Luo, B., Tsias, A., Peter, T., 2000. Water activity as the determinant for homogeneous
1034 ice nucleation in aqueous solutions. Nature 406, 611-614.
- 1035 Liao, H., Henze, D.K., Seinfeld, J.H., Wu, S., Mickley, L.J., 2007. Biogenic secondary organic
1036 aerosol over the United States: Comparison of climatological simulations with observations.
1037 Journal of Geophysical Research 112, D06201.

- 1038 Liu, H., Jacob, D.J., Bey, I., Yantosca, R.M., 2001. Constraints from ^{210}Pb and ^7Be on wet
1039 deposition and transport in a global three-dimensional chemical tracer model driven by
1040 assimilated meteorological fields. *Journal of Geophysical Research* 106, 12109-12128.
- 1041 Liu, H., Jacob, D.J., Bey, I., Yantosca, R.M., Duncan, B.N., Sachse, G.W., 2003. Transport
1042 pathways for Asian pollution outflow over the Pacific: Interannual and seasonal variations.
1043 *Journal of Geophysical Research* 108, 8786.
- 1044 Lowenthal, D.H., Rahn, K.A., 1985. Regional sources of pollution aerosol at Barrow, Alaska
1045 during winter 1979-80 as deduced from elemental tracers. *Atmospheric Environment* 19, 2011-
1046 2024.
- 1047 Lubin, D., Vogelmann, A.M., 2006. A climatologically significant aerosol longwave indirect
1048 effect in the Arctic. *Nature* 439, 453-456.
- 1049 Lubin, D., Vogelmann, A.M., 2007. Expected magnitude of the aerosol shortwave indirect effect
1050 in springtime Arctic liquid water clouds. *Geophysical Research Letters* 34, L11801.
- 1051 Malm, W.C., Sisler, J.F., Huffman, D., Eldred, R.A., Cahill, T.A., 1994. Spatial and seasonal
1052 trends in particle concentration and optical extinction in the United States. *Journal of*
1053 *Geophysical Research* 99, 1347-1370.
- 1054 Mao, J., Jacob, D.J., Evans, M.J., Olson, J.R., Ren, X., Brune, W.H., St. Clair, J.M., Crouse,
1055 J.D., Spencer, K.M., Beaver, M.R., Wennberg, P.O., Cubison, M.J., Jimenez, J.L., Fried, A.,
1056 Weibring, P., Walega, J.G., Hall, S.R., Weinheimer, A.J., Cohen, R.C., Chen, G., Crawford, J.H.,
1057 McNaughton, C., Clarke, A.D., Jaeglé, L., Fisher, J.A., Yantosca, R.M., Le Sager, P., Carouge,
1058 C., 2010. Chemistry of hydrogen oxide radicals (HOx) in the Arctic troposphere in spring.
1059 *Atmospheric Chemistry and Physics* 10, 5823-5838.
- 1060 Martin, S.T., Hung, H.M., Park, R.J., Jacob, D.J., Spurr, R.J.D., Chance, K.V., Chin, M., 2004.
1061 Effects of the physical state of tropospheric ammonium-sulfate-nitrate particles on global aerosol
1062 direct radiative forcing. *Atmospheric Chemistry and Physics* 4, 183-214.
- 1063 McNaughton, C.S., Clarke, A.D., Kapustin, V., Shinozuka, Y., Howell, S.G., Anderson, B.E.,
1064 Winstead, E., Dibb, J., Scheuer, E., Cohen, R.C., Wooldridge, P., Perring, A., Huey, L.G., Kim,
1065 S., Jimenez, J.L., Dunlea, E.J., DeCarlo, P.F., Wennberg, P.O., Crouse, J.D., Weinheimer, A.,
1066 Flocke, F., 2009. Observations of heterogeneous reactions between Asian pollution and mineral
1067 dust over the Eastern North Pacific during INTEX-B. *Atmospheric Chemistry and Physics* 9,
1068 8283-8208.
- 1069 Mensah, A.A., Buchholz, A., Mentel, T.F., Tillmann, R., Kiendler-Scharr, A., 2011. Aerosol
1070 mass spectrometric measurements of stable crystal hydrates of oxalates and inferred relative
1071 ionization efficiency of water. *Journal of Aerosol Science* 42, 11-19.
- 1072 Murakami, M., Kimura, T., Magono, C., Kikuchi, K., 1983. Observations of precipitation
1073 scavenging for water-soluble particles. *Journal of the Meteorological Society of Japan* 61, 346-
1074 358.

- 1075 National Atmospheric Deposition Program, 2010. NADP Program Office, Illinois State Water
1076 Survey, Champaign, IL.
- 1077 Nilsson, E.D., Rannik, Ü., 2001. Turbulent aerosol fluxes over the Arctic Ocean: 1. Dry
1078 deposition over sea and pack ice. *Journal of Geophysical Research* 106, 32125-32137.
- 1079 Olivier, J.G.J., Bloos, J.P.J., Berdowski, J.J.M., Visschedijk, A.J.H., Bouwman, A.F., 1999. A
1080 1990 global emission inventory of anthropogenic sources of carbon monoxide on 1° x 1°
1081 developed in the framework of EDGAR/GEIA. *Chemosphere: Global Change Science* 1, 1-17.
- 1082 Park, R.J., Jacob, D.J., Field, B.D., Yantosca, R.M., Chin, M., 2004. Natural and transboundary
1083 pollution influences on sulfate-nitrate-ammonium aerosols in the United States: Implications for
1084 policy. *Journal of Geophysical Research* 109, D15204.
- 1085 Parungo, F., Nagamoto, C., Herbert, G., Harris, J., Schnell, R., Sheridan, P., Zhang, N., 1993.
1086 Individual particle analyses of Arctic aerosol samples collected using AGASP-III. *Atmospheric
1087 Environment* 27A, 2825-2837.
- 1088 Piot, M., von Glasow, R., 2008. The potential importance of frost flowers, recycling on snow,
1089 and open leads for ozone depletion events. *Atmospheric Chemistry and Physics* 8, 2437-2467.
- 1090 Prank, M., Sofiev, M., Denier van der Gon, H.A.C., Kaasik, M., Ruuskanen, T.M., Kukkonen, J.,
1091 2010. A refinement of the emission data for Kola Peninsula based on inverse dispersion
1092 modelling. *Atmospheric Chemistry and Physics* 10, 10849-10865.
- 1093 Pueschel, R.F., Kinne, S.A., 1995. Physical and radiative properties of Arctic atmospheric
1094 aerosols. *The Science of the Total Environment* 160/161, 811-824.
- 1095 Pye, H., Liao, H., Wu, S., Mickley, L., Jacob, D., Henze, D., Seinfeld, J., 2009. Effect of changes
1096 in climate and emissions on future sulfate-nitrate-ammonium aerosol levels in the United States.
1097 *Journal of Geophysical Research* 114, D01205.
- 1098 Quinn, P.K., Bates, T.S., Baum, E., Doubleday, N., Fiore, A.M., Flanner, M., Fridlind, A.,
1099 Garrett, T.J., Koch, D., Menon, S., 2008. Short-lived pollutants in the Arctic: their climate
1100 impact and possible mitigation strategies. *Atmospheric Chemistry and Physics* 8, 1723-1735.
- 1101 Quinn, P.K., Bates, T.S., Schulz, K., Shaw, G.E., 2009. Decadal trends in aerosol chemical
1102 composition at Barrow, Alaska: 1976-2008. *Atmospheric Chemistry and Physics* 9, 8883-8888.
- 1103 Quinn, P.K., Miller, T.L., Bates, T.S., Ogren, J.A., Andrews, E., Shaw, G.E., 2002. A 3-year
1104 record of simultaneously measured aerosol chemical and optical properties at Barrow, Alaska.
1105 *Journal of Geophysical Research* 107, 4130.
- 1106 Quinn, P.K., Shaw, G., Andrews, E., Dutton, E.G., Ruoho-Airola, T., Gong, S.L., 2007. Arctic
1107 haze: current trends and knowledge gaps. *Tellus B* 59, 99-114.
- 1108 Raatz, W.E., Shaw, G.E., 1984. Long-Range Tropospheric Transport of Pollution Aerosols into
1109 the Alaskan Arctic. *Journal of Applied Meteorology* 23, 1052-1064.

- 1110 Rahn, K.A., 1981a. Relative importances of North America and Eurasia as sources of arctic
1111 aerosol. *Atmospheric Environment* 15, 1447-1455.
- 1112 Rahn, K.A., 1981b. The Mn/V ratio as a tracer of large-scale sources of pollution aerosol for the
1113 Arctic. *Atmospheric Environment* 15, 1457-1464.
- 1114 Rahn, K.A., Lewis, N.F., Lowenthal, D.H., Smith, D.L., 1983. Noril'sk only a minor contributor
1115 to Arctic haze. *Nature* 306, 459-461.
- 1116 Rastigejev, Y., Park, R., Brenner, M.P., Jacob, D.J., 2010. Resolving intercontinental pollution
1117 plumes in global models of atmospheric transport. *Journal of Geophysical Research* 115,
1118 D02302.
- 1119 Reid, J.S., Hyer, E.J., Prins, E.M., Westphal, D.L., Zhang, J., Wang, J., Christopher, S.A., Curtis,
1120 C.A., Schmidt, C.C., Eleuterio, D.P., Richardson, K.A., Hoffman, J.P., 2009. Global monitoring
1121 and forecasting of biomass-burning smoke: Description and lessons from the Fire Locating and
1122 Modeling of Burning Emissions (FLAMBE) program. *IEEE Journal of Selected Topics in*
1123 *Applied Earth Observations and Remote Sensing* 2, 144-162.
- 1124 Reis, S., Pinder, R.W., Zhang, M., Lijie, G., Sutton, M.A., 2009. Reactive nitrogen in
1125 atmospheric emission inventories. *Atmospheric Chemistry and Physics* 9, 7647-7677.
- 1126 Ritter, C., Notholt, J., Fischer, J., Rathke, C., 2005. Direct thermal radiative forcing of
1127 tropospheric aerosol in the Arctic measured by ground based infrared spectrometry. *Geophysical*
1128 *Research Letters* 32, L23816.
- 1129 Scheuer, E., Talbot, R.W., Dibb, J.E., Seid, G.K., DeBell, L., Lefer, B., 2003. Seasonal
1130 distributions of fine aerosol sulfate in the North American Arctic basin during TOPSE. *Journal*
1131 *of Geophysical Research* 108, 8370.
- 1132 Seinfeld, J.H., Pandis, S.N., 2006. *Atmospheric Chemistry and Physics: From Air Pollution to*
1133 *Climate Change*, 2nd ed. John Wiley, New York.
- 1134 Sharma, S., Andrews, E., Barrie, L.A., Ogren, J.A., Lavoué, D., 2006. Variations and sources of
1135 the equivalent black carbon in the high Arctic revealed by long-term observations at Alert and
1136 Barrow: 1989–2003. *J. Geophys. Res.* 111, D14208.
- 1137 Sharma, S., Lavoué, D., Cachier, H., Barrie, L.A., Gong, S.L., 2004. Long-term trends of the
1138 black carbon concentrations in the Canadian Arctic. *J. Geophys. Res.-Atmos.* 109, D15203.
- 1139 Shaw, G.E., 1995. The Arctic haze phenomenon. *Bulletin of the American Meteorological*
1140 *Society* 76, 2403-2413.
- 1141 Sheridan, P.J., Musselman, I.H., 1985. Characterization of aircraft-collected particles present in
1142 the arctic aerosol: Alaskan Arctic, spring 1983. *Atmospheric Environment* 19, 2159-2166.
- 1143 Shindell, D.T., Chin, M., Dentener, F., Doherty, R.M., Faluvegi, G., Fiore, A.M., Hess, P., Koch,
1144 D.M., MacKenzie, I.A., Sanderson, M.G., Schultz, M.G., Schulz, M., Stevenson, D.S., Teich, H.,

- 1145 Textor, C., Wild, O., Bergmann, D.J., Bey, I., Bian, H., Cuvelier, C., Duncan, B.N., Folberth, G.,
1146 Horowitz, L.W., Jonson, J., Kaminski, J.W., Marmer, E., Park, R., Pringle, K.J., Schroeder, S.,
1147 Szopa, S., Takemura, T., Zeng, G., Keating, T.J., Zuber, A., 2008. A multi-model assessment of
1148 pollution transport to the Arctic. *Atmospheric Chemistry and Physics* 8, 5353-5372.
- 1149 Shindell, D.T., Faluvegi, G., 2009. Climate response to regional radiative forcing during the
1150 twentieth century. *Nature Geoscience* 2, 294-300.
- 1151 Smith, S.J., van Aardenne, J., Klimont, Z., Andres, R., Volke, A., Delgado Arias, S., 2010.
1152 Anthropogenic sulfur dioxide emissions: 1850-2005. *Atmospheric Chemistry and Physics*
1153 *Discussions* 10, 1611-16151.
- 1154 Stephens, G.L., L'Ecuyer, T., Forbes, R., Gettleman, A., Golaz, J.-C., Bodas-Salcedo, A., Suzuki,
1155 K., Gabriel, P., Haynes, J., 2010. Dreary state of precipitation in global models. *Journal of*
1156 *Geophysical Research* 115, D24211.
- 1157 Stohl, A., 2006. Characteristics of atmospheric transport into the Arctic troposphere. *Journal of*
1158 *Geophysical Research* 111, D11306.
- 1159 Streets, D.G., Bond, T.C., Carmichael, G.R., Fernandes, S.D., Fu, Q., He, D., Klimont, Z.,
1160 Nelson, S.M., Tsai, N.Y., Wang, M.Q., 2003. An inventory of gaseous and primary aerosol
1161 emissions in Asia in the year 2000. *Journal of Geophysical Research* 108, 8809.
- 1162 Tarrasón, L., Iversen, T., 1998. Modelling intercontinental transport of atmospheric sulphur in
1163 the northern hemisphere. *Tellus* 50B, 331-352.
- 1164 Toom-Sauntry, D., Barrie, L.A., 2002. Chemical composition of snowfall in the high Arctic:
1165 1990-1994. *Atmospheric Environment* 36, 2683-2893.
- 1166 Trenberth, K.E., Jones, P.D., Ambenje, P., Bojariu, R., Easterling, D., Klein Tank, A., Parker,
1167 D., Rahimzadeh, F., Renwick, J.A., Rusticucci, M., Soden, B., Zhai, P., 2007. Observations:
1168 Surface and Atmospheric Change, in: Solomon, S., Qin, D., Manning, M., Chen, Z., Averyt,
1169 K.B., Tignor, M., Miller, H.L. (Eds.), *Climate Change 2007: The Physical Science Basis.*
1170 *Contribution of Working Group I to the Fourth Assessment Report of the Intergovernmental*
1171 *Panel on Climate Change.* Cambridge University Press, Cambridge, United Kingdom and New
1172 York, NY USA.
- 1173 Vestreng, V., Klein, H., 2002. Emission data reported to UNECE/EMEP: quality assurance and
1174 trend analysis & presentation of WebDab. Norwegian Meteorological Institute, Oslo, Norway.
- 1175 Wang, J., Hoffmann, A.A., Park, R.J., Jacob, D.J., Martin, S.T., 2008a. Global distribution of
1176 solid and aqueous sulfate aerosols: Effect of the hysteresis of particle phase transitions. *Journal*
1177 *of Geophysical Research* 113, D11206.
- 1178 Wang, J., Jacob, D.J., Martin, S.T., 2008b. Sensitivity of sulfate direct climate forcing to the
1179 hysteresis of particle phase transitions. *J. Geophys. Res.* 113.

1180 Wang, Q., Jacob, D.J., Fisher, J.A., Mao, J., Le Sager, P., Leibensperger, E.M., Carouge, C.,
1181 Kondo, Y., Jimenez, J.L., Cubison, M.J., Howell, S.G., Freitag, S., Clarke, A.D., McNaughton,
1182 C.S., Weber, R., Apel, E.C., 2011. Sources of carbonaceous aerosols and deposited black carbon
1183 in the Arctic in spring. in preparation.

1184 Wang, Y., Jacob, D.J., Logan, J.A., 1998. Global simulation of tropospheric O₃-NO_x-
1185 hydrocarbon chemistry: 1. Model formulation. *Journal of Geophysical Research* 103, 10713-
1186 10725.

1187 Warneke, C., Bahreini, R., Brioude, J., Brock, C.A., de Gouw, J.A., Fahey, D.W., Froyd, K.D.,
1188 Holloway, J.S., Middlebrook, A., Miller, L., Montzka, S., Murphy, D.M., Peischl, J., Ryerson,
1189 T.B., Schwarz, J.P., Spackman, J.R., Veres, P., 2009. Biomass burning in Siberia and
1190 Kazakhstan as the main source for Arctic Haze over the Alaskan Arctic in April 2008.
1191 *Geophysical Research Letters* 36, L02813.

1192 Warneke, C., Froyd, K.D., Brioude, J., Bahreini, R., Brock, C.A., Cozic, A., de Gouw, J.A.,
1193 Fahey, D.W., Ferrare, R.A., Holloway, J.S., Middlebrook, A.M., Miller, L., Montzka, S.,
1194 Schwarz, J.P., Sodemann, H., Spackman, J.R., Stohl, A., 2010. An important contribution to
1195 springtime Arctic aerosol from biomass burning in Russia. *Geophysical Research Letters* 37,
1196 L01801.

1197 Wesely, M.L., 1989. Parameterization of surface resistances to gaseous dry deposition in
1198 regional-scale numerical models. *Atmospheric Environment* 23, 1293-1304.

1199 Wise, M.E., Baustian, K.J., Tolbert, M.A., 2009. Laboratory studies of ice formation pathways
1200 from ammonium sulfate particles. *Atmospheric Chemistry and Physics* 9, 1639-1646.

1201 Yamagata, S., Kobayashi, D., Ohta, S., Murao, N., Shiobara, M., Wada, M., Yabuki, M.,
1202 Konishi, H., Yamanouchi, T., 2009. Properties of aerosols and their wet deposition in the arctic
1203 spring during ASTAR2004 at Ny-Alesund, Svalbard. *Atmospheric Chemistry and Physics* 9,
1204 261-270.

1205 Zhang, Q., Jimenez, J.L., Worsnop, D.R., Canagaratna, M., 2007a. A case study of urban particle
1206 acidity and its influence on secondary organic aerosol. *Environmental Science & Technology* 41,
1207 3213-3219.

1208 Zhang, Q., Streets, D.G., Carmichael, G.R., He, K.B., Huo, H., Kannari, A., Klimont, Z., Park,
1209 I.S., Reddy, S., Fu, J.S., Chen, D., Duan, L., Lei, Y., Wang, L.T., Yao, Z.L., 2009. Asian
1210 emissions in 2006 for the NASA INTEX-B mission. *Atmospheric Chemistry and Physics* 9,
1211 5131-5153.

1212 Zhang, Q., Streets, D.G., He, K., Wang, Y., Richter, A., Burrows, J.P., Uno, I., Jang, C.J., Chen,
1213 D., Yao, Z., 2007b. NO_x emission trends for China, 1995-2004: The view from the ground and
1214 the view from space. *Journal of Geophysical Research* 112, D22306.
1215
1216

1217 **Figure captions**

1218 **Figure 1.** January-May 2008 GEOS-Chem emissions of (a) SO₂ (kg S km⁻²) and (b) NH₃ (kg N
1219 km⁻²), averaged over the 2°x2.5° model grid. Regional totals are given in Table 1.

1220 **Figure 2.** (a) Sulfate and (b) ammonium wet deposition fluxes over North America, Europe, and
1221 East Asia in April 2008. Model results (background) are compared to observations (circles) from
1222 the NADP, EMEP, and EANET networks. Major outliers in the observations (sulfate deposition
1223 > 4 kg ha⁻¹, ammonium deposition > 1.5 kg ha⁻¹) are highlighted in white trim. Correlation
1224 coefficients (*r*) and normalized mean biases (NMB), computed after removing major outliers, are
1225 given inset. Mean observed pH for each network (computed by averaging the mean precipitation-
1226 weighted [H⁺] at each site) is also given inset.

1227 **Figure 3.** Regions used for source attribution of sulfate-ammonium aerosol in the Arctic. Model
1228 sensitivity simulations were conducted with anthropogenic emissions from each of these regions
1229 shut off individually. Additional sensitivity simulations were conducted shutting off global ship,
1230 biomass burning and natural emissions. Also shown are the flight tracks for ARCTAS (brown)
1231 and ARCPAC (yellow) and the locations of surface stations used for model evaluation: Alert
1232 (A), Barrow (B), Denali (D), and Zeppelin (Z).

1233 **Figure 4.** Comparison of modeled and observed (a) sulfate and (b) ammonium during ARCTAS
1234 (top) and ARCPAC (bottom), colored by altitude. Biomass burning plumes, stratospheric air,
1235 local pollution, observations south of 60°N, and major outliers have been removed from the
1236 comparisons as described in the text. All concentrations are reported in nmol m⁻³ at standard
1237 temperature and pressure (STP). Also shown are the 1:1 lines (dashed) and reduced-major-axis
1238 regression lines (solid). Correlation coefficients (*r*) and normalized mean biases (NMB) are
1239 given inset. There are many more comparison points for ARCPAC than ARCTAS, despite fewer
1240 flight hours and smaller sampling domain, because of the long integration time (4-24 minutes) of
1241 the SAGA filters on the ARCTAS aircraft.

1242 **Figure 5.** Mean vertical distributions of (a) sulfate and (b) ammonium during ARCTAS (top)
1243 and ARCPAC (bottom). Dark gray bars show mean observed concentrations, and colored bars
1244 show mean model results. Modeled concentrations are decomposed into contributions from
1245 various sources as indicated in the legend. Biomass burning refers to open biomass burning;
1246 biofuel is included in the anthropogenic source. The “other” anthropogenic term also includes
1247 minor non-linear effects in source attribution (see text). Biomass burning plumes, stratospheric
1248 air, local pollution, observations south of 60°N, and major outliers have been removed from the
1249 data as described in the text.

1250 **Figure 6.** January-May monthly mean (a) sulfate and (b) ammonium concentrations observed
1251 and modeled at Arctic surface sites. No ammonium data are available at Denali or other
1252 IMPROVE sites. The thick black lines show the observed 2004-2008 monthly means and
1253 interannual standard deviations; 2008 monthly means are shown as thin lines. Modeled
1254 concentrations are subdivided into contributions from individual sources as indicated in the
1255 legend. Biomass burning refers to open biomass burning; biofuel is included in the
1256 anthropogenic source. The “other” anthropogenic term also includes minor non-linear effects in
1257 source attribution (see text). Data sources are as follows: Alert – Environment Canada (Gong et
1258 al., 2010); Zeppelin – EMEP (<http://ebas.nilu.no>); Barrow – the NOAA Pacific Marine

1259 Environmental Laboratory (<http://saga.pmel.noaa.gov/data/>); Denali - the IMPROVE network
1260 (Malm et al., 1994).

1261 **Figure 7.** GEOS-Chem budgets of sulfate and ammonium aerosols in the High Arctic (75-90°N)
1262 in (a) April 2008 and (b) January-February 2008. Aerosol concentrations from 10 different
1263 sources are shown for three altitude bands. Biomass burning refers to open biomass burning;
1264 biofuel is included in the anthropogenic source. The “other” anthropogenic term also includes
1265 minor non-linear effects in source attribution (see text).

1266 **Figure 8.** Scatterplots of (a) observed and (b) modeled acid aerosol neutralization during
1267 ARCTAS and ARCPAC, as given by the $2[\text{SO}_4^{2-}] + [\text{NO}_3^-]$ vs. $[\text{NH}_4^+]$ relationship. Dashed lines
1268 indicate the degree of aerosol neutralization, with fully neutralized aerosols falling along the $f =$
1269 1 line.

1270 **Figure 9.** Scatterplot of the aerosol neutralization fraction for aerosol originating from the four
1271 major anthropogenic source regions in the GEOS-Chem simulation of the ARCTAS and
1272 ARCPAC aircraft data in April 2008. Colored lines show the reduced-major-axis linear
1273 regressions. Dashed lines indicate the $f = 0.5$ and $f = 1$ lines, as in Fig. 8.

1274 **Figure 10.** 2004-2008 monthly means and interannual standard deviations of aerosol neutralized
1275 fraction ($f = [\text{NH}_4^+] / (2[\text{SO}_4^{2-}] + [\text{NO}_3^-])$) observed at Zeppelin (blue), Barrow (purple), and Alert
1276 (red).

1277 **Figure 11.** Maps of mean aerosol neutralized fraction ($f = [\text{NH}_4^+] / (2[\text{SO}_4^{2-}] + [\text{NO}_3^-])$) simulated
1278 by GEOS-Chem in surface air and at 5 km altitude for April and January-February 2008. The
1279 black dashed line marks the limit of the High Arctic at 75°N.

Table 1. Global SO₂ and NH₃ emissions for 2008.^a

Source	SO ₂ , Tg S	NH ₃ , Tg N
Anthropogenic ^b	64 (27)	39 (15)
Contiguous U.S. and Canada (south of 60°N)	8.0 (3.3) ^{c,d}	2.6 (0.82) ^d
Europe (south of 60°N)	6.9 (3.2) ^e	5.2 (2.3) ^e
West Asia and Siberia (south of 60°N)	3.3 (1.4)	1.2 (0.30)
East Asia	23 (9.7) ^f	21 (7.4) ^g
North American Arctic (60-90°N, 180-37.5°W)	0.016 (0.0067) ^d	0.0015 (0.0006) ^d
Eurasian Arctic (60-90°N, 37.5°W-180°E)	0.58 (0.25) ^e	0.14 (0.049) ^e
Rest of world	13 (5.3)	8.5 (3.8)
Ships	8.5 (3.5) ^h	
Aircraft	0.070 (0.028) ⁱ	--
Open Biomass burning ^j	2.0 (0.56) ^k	9.5 (2.3) ^k
Natural sources	31 (13)	14.3 (5.9)
Oxidation of biogenic dimethyl sulfide (DMS)	18 (8.1) ^l	--
Volcanism	13 (5.1) ^m	--
Ocean, soil, crop decomposition, wild animals	--	14.3 (5.9) ⁿ
TOTAL	97 (41)	62 (23)

^a Annual totals for 2008 used in GEOS-Chem. Totals for January-May are given in parentheses.

^b Including fuel and industrial emissions of SO₂ and agricultural and fuel emissions of NH₃. Fuel emissions are mostly from coal for SO₂ and from biomass (biofuel) for NH₃. Default anthropogenic emission inventories are EDGAR 3.2 for SO₂ in 2000 (Olivier et al., 1999) and the Bouwman et al. (1997) implementation of the Global Emissions Inventory Activity (GEIA) for NH₃ in 1990 with seasonality from Park et al. (2004). These inventories are overwritten for specific regions as indicated in footnotes. See Fig. 3 for region definitions.

^c U.S. anthropogenic SO₂ emissions are from the US Environmental Protection Agency National Emission Inventory for 1999 (EPA-NEI99, <http://www.epa.gov/ttnchie1/net/1999inventory.html>).

^d Canadian anthropogenic emissions are from the Criteria Air Contaminants (CAC) inventory for 2005 (Environment Canada, http://www.ec.gc.ca/pdb/cac/cac_home_e.cfm).

^e European anthropogenic emissions are from the Cooperative Programme for Monitoring and Evaluation of the Long-range Transmission of Air Pollutants in Europe (EMEP) inventory for 2005 (Vestreng and Klein, 2002). These are also used for the European Arctic, while EDGAR 3.2 is used for the Asian Arctic in the absence of better information.

^f Asian SO₂ emissions are from the NASA INTEX-B inventory for 2006 (Zhang et al., 2009) with seasonality based on monthly NO_x emissions (Zhang et al., 2007b).

^g East Asian annual NH₃ emissions are from Streets et al. (2003) with superimposed relative seasonal variation based on the length of the growing season for fertilizer use and on temperature and wind speed for everything else (L. Bouwman, personal communication).

^h Ship emissions of SO₂ are based on EDGAR 2000 (Eyring et al., 2005a; Eyring et al., 2005b), overwritten over Europe by the EMEP inventory.

ⁱ Aircraft emissions of SO₂ are based on mean fuel consumption from the NASA Atmospheric Effects of Aviation Project (Baughcum et al., 1996) as described by Chin et al. (2000).

^j Excluding biofuel, which is included in the anthropogenic source.

^k Biomass burning emissions are from the FLAMBE inventory (Reid et al., 2009) corrected by Fisher et al. (2010), and are computed as described in the text.

^l The source from DMS oxidation is as described by Park et al. (2004).

^m Volcanic SO₂ emissions are from the AEROCOM inventory (Diehl, 2009). Emissions from continuous (non-eruptive) volcanic degassing are injected at the altitude of the volcanic crater. Eruptive emissions are emitted evenly over the top third of the volcanic plume, as described by Chin et al. (2000).

ⁿ Natural NH₃ emissions (ocean, soil, crop decomposition, and wild animals) are from Bouwman et al. (1997).

Table 2. Sulfate neutralization ratios by source region.^a

Region ^b	Emissions ^c $E_{NH_3}/2E_{SO_2}$ (mol mol ⁻¹)	Wet deposition (source region) ^d $[NH_4^+]/(2[SO_4^{2-}])$ (mol mol ⁻¹)	
		Observations	Model
East Asia	1.2	0.76	0.87
Europe	1.3	1.4	1.7
North America	0.29	0.76	0.45
West Asia	0.23	--	

^a Values are for April 2008^b Region definitions are given in Fig. 3.^c Ratio of regional emissions as given in Table 1, for April only.^d Ratios of mean precipitation-weighted concentrations at the NADP, EMEP, and non-urban EANET sites.

Figure1

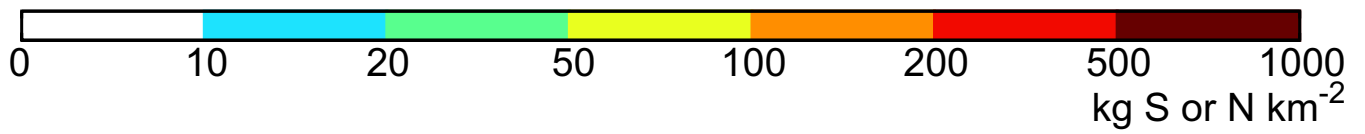
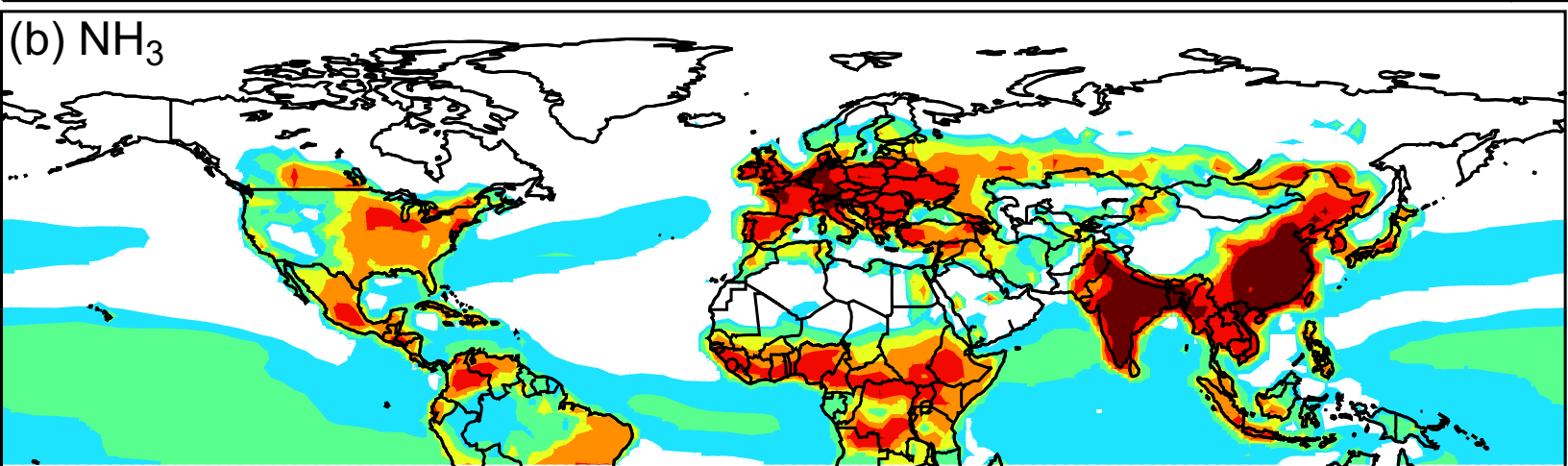
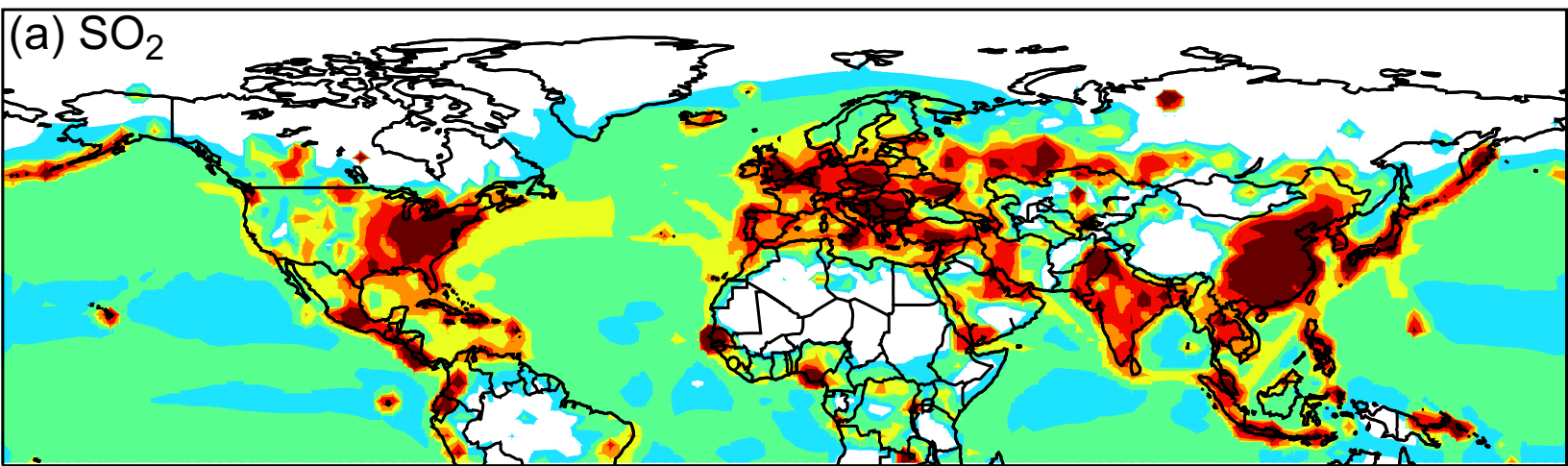


Figure2

(a) Sulfate

(b) Ammonium

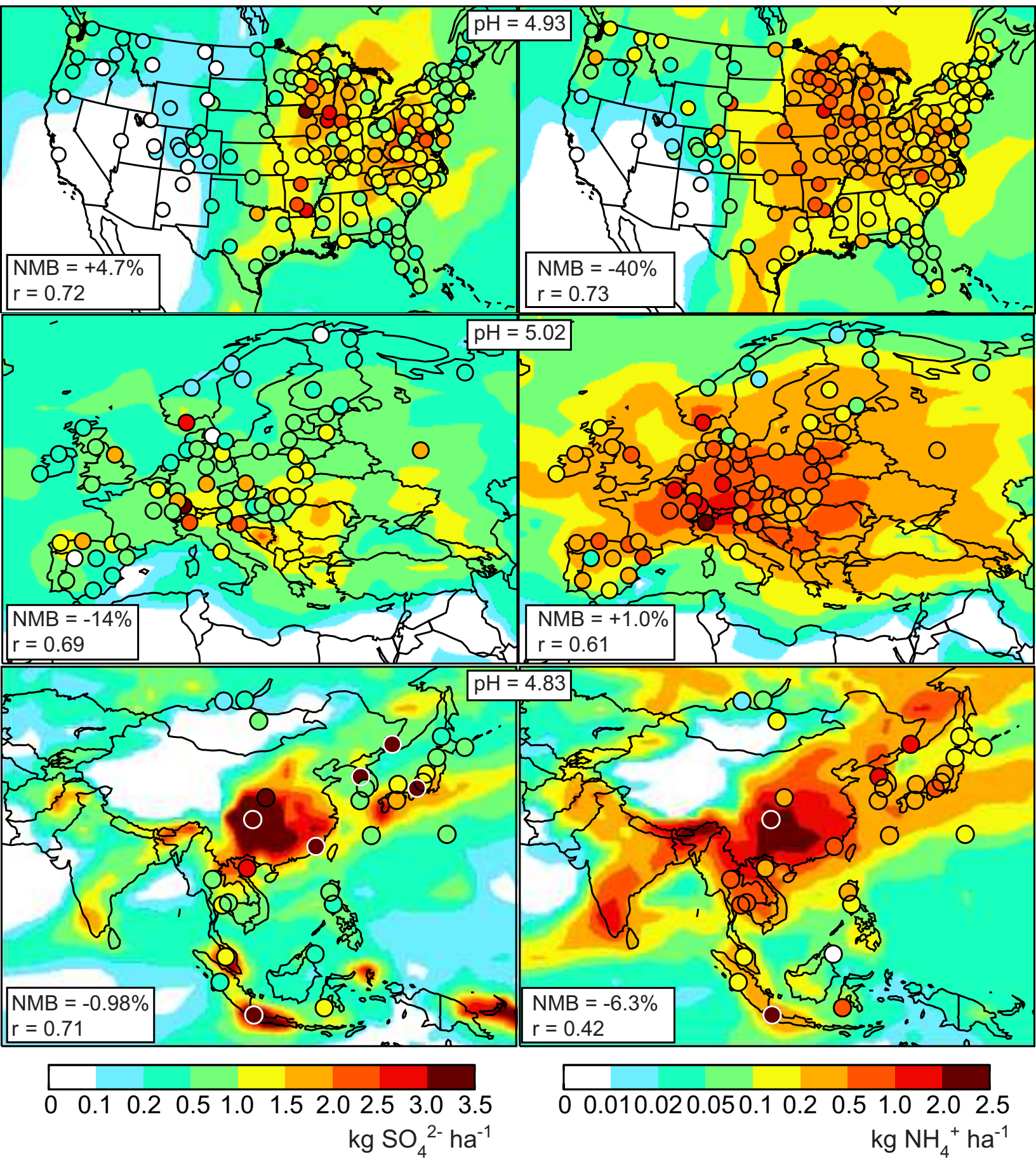


Figure3

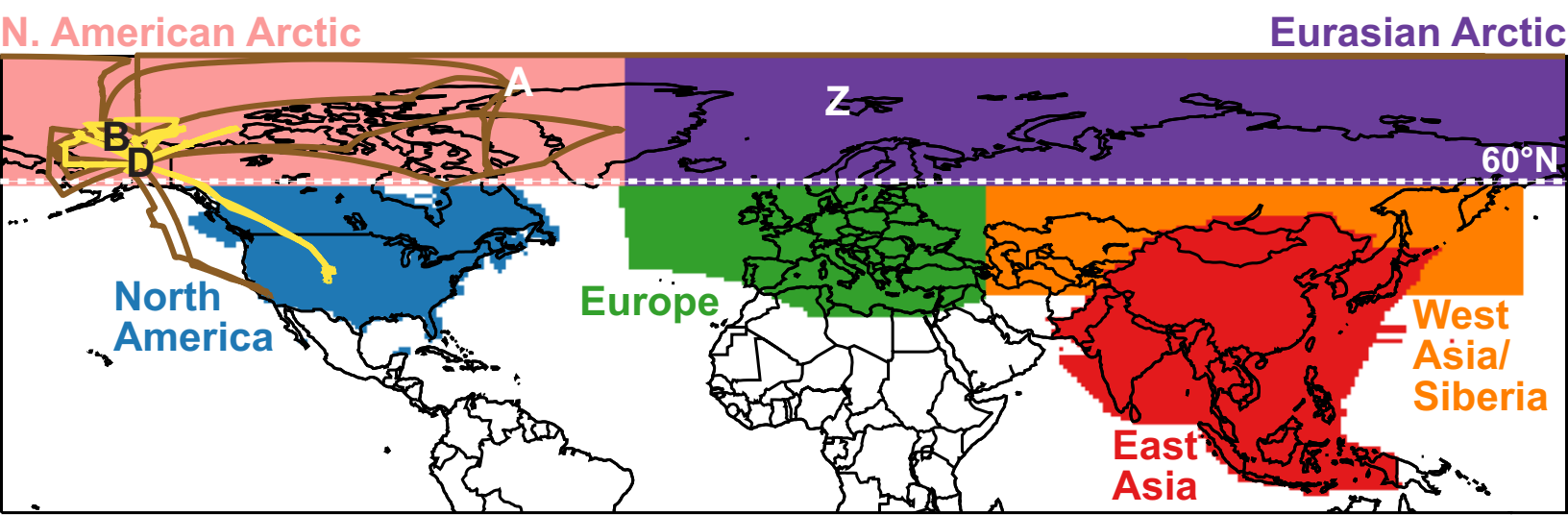


Figure 4

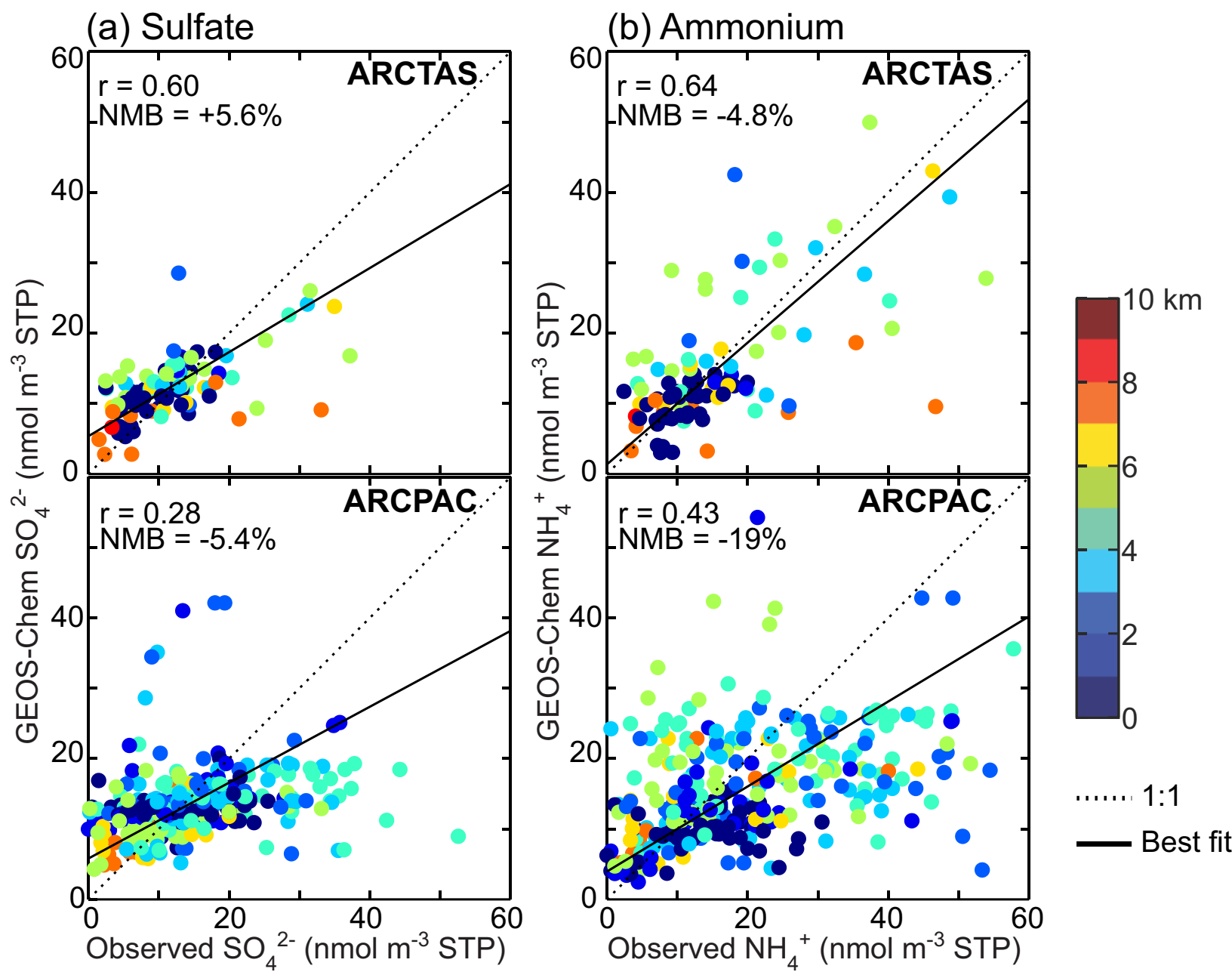


Figure5

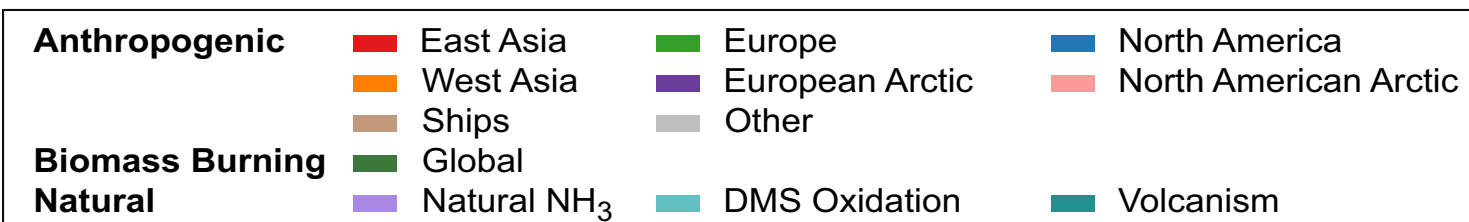
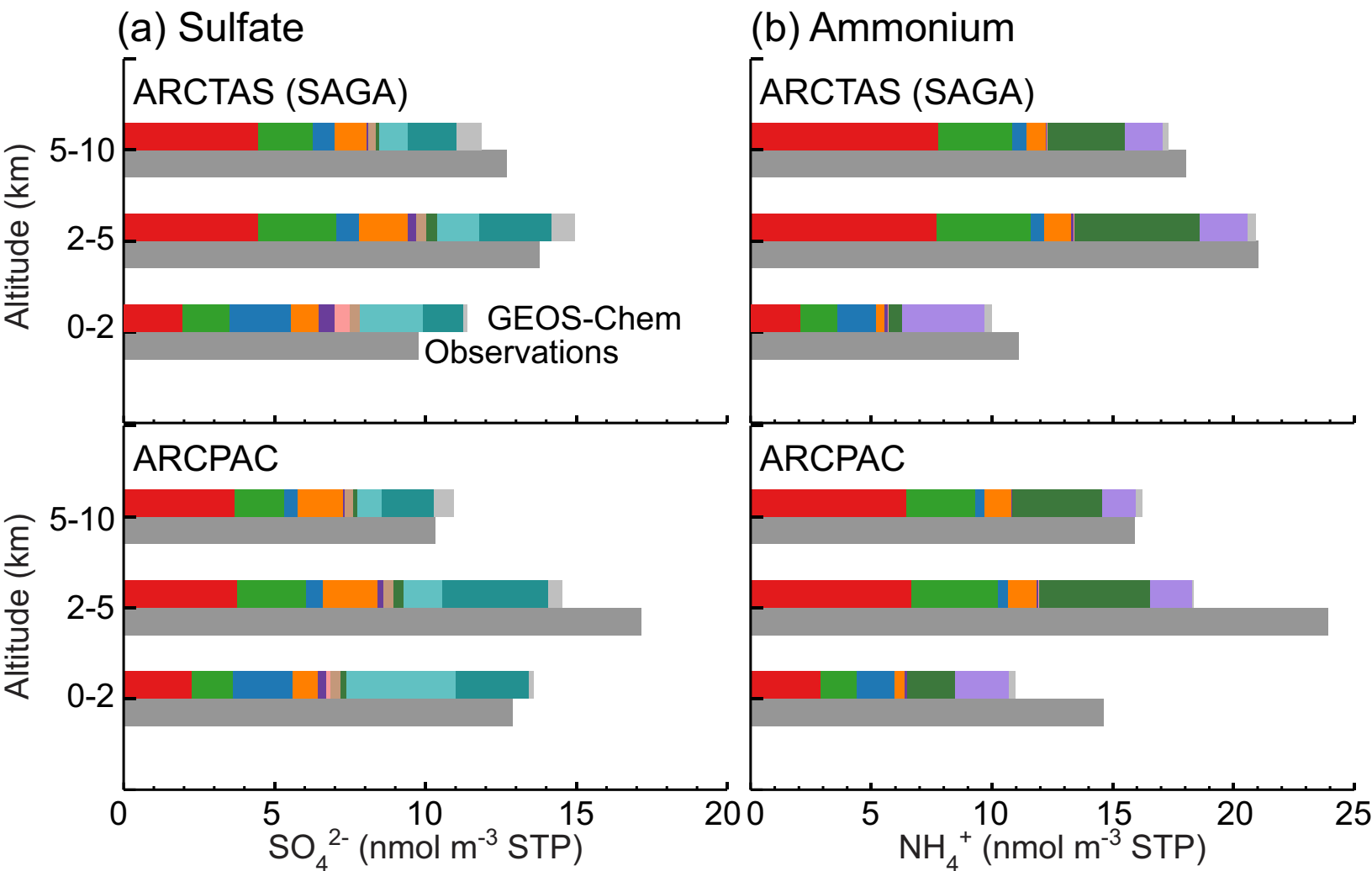


Figure 6

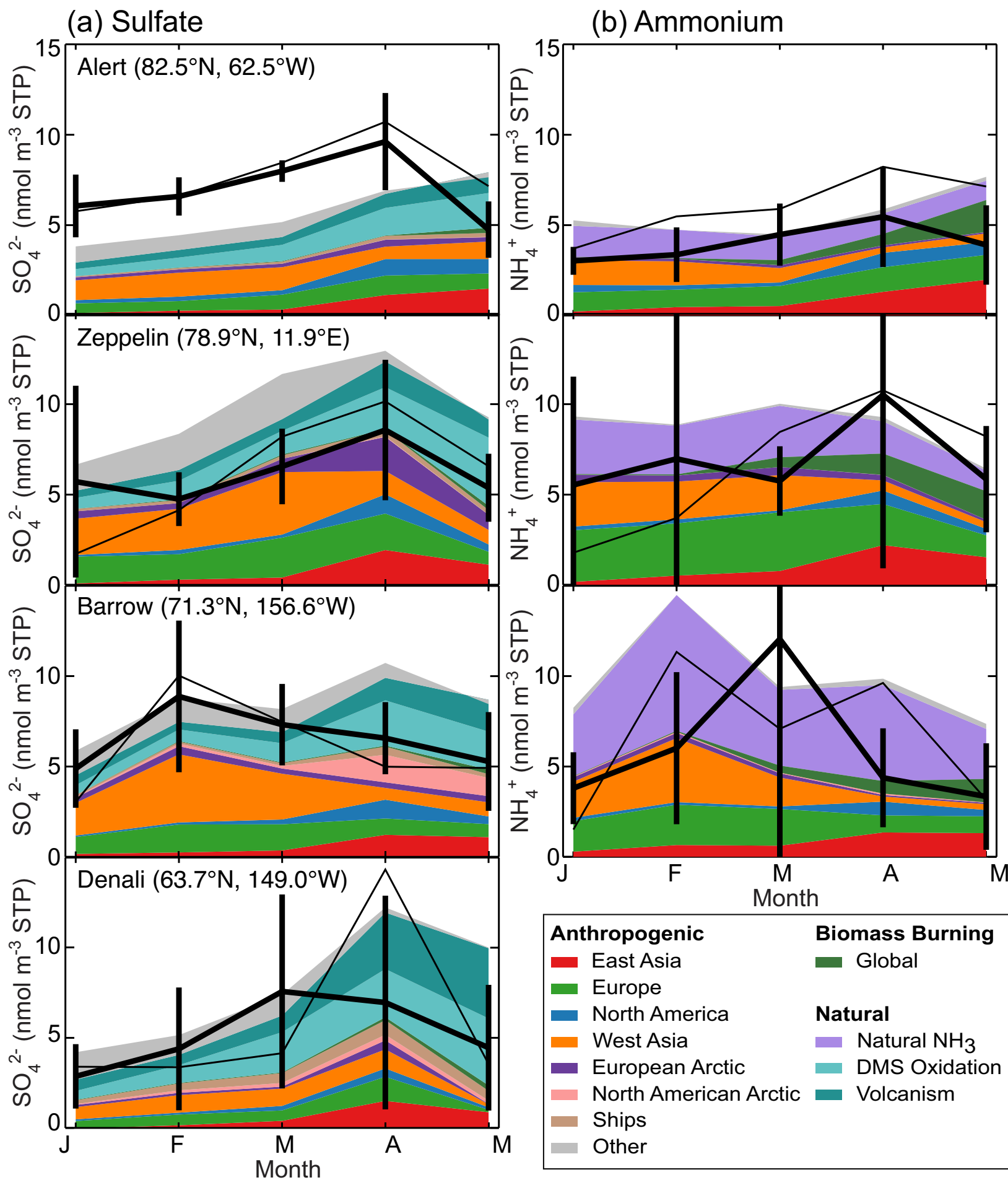


Figure 7

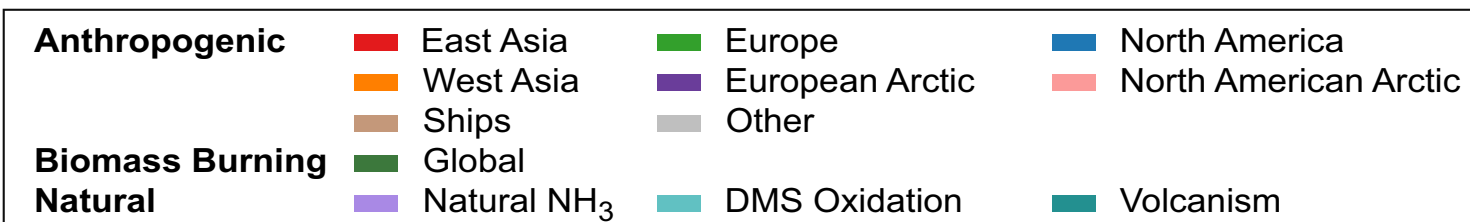
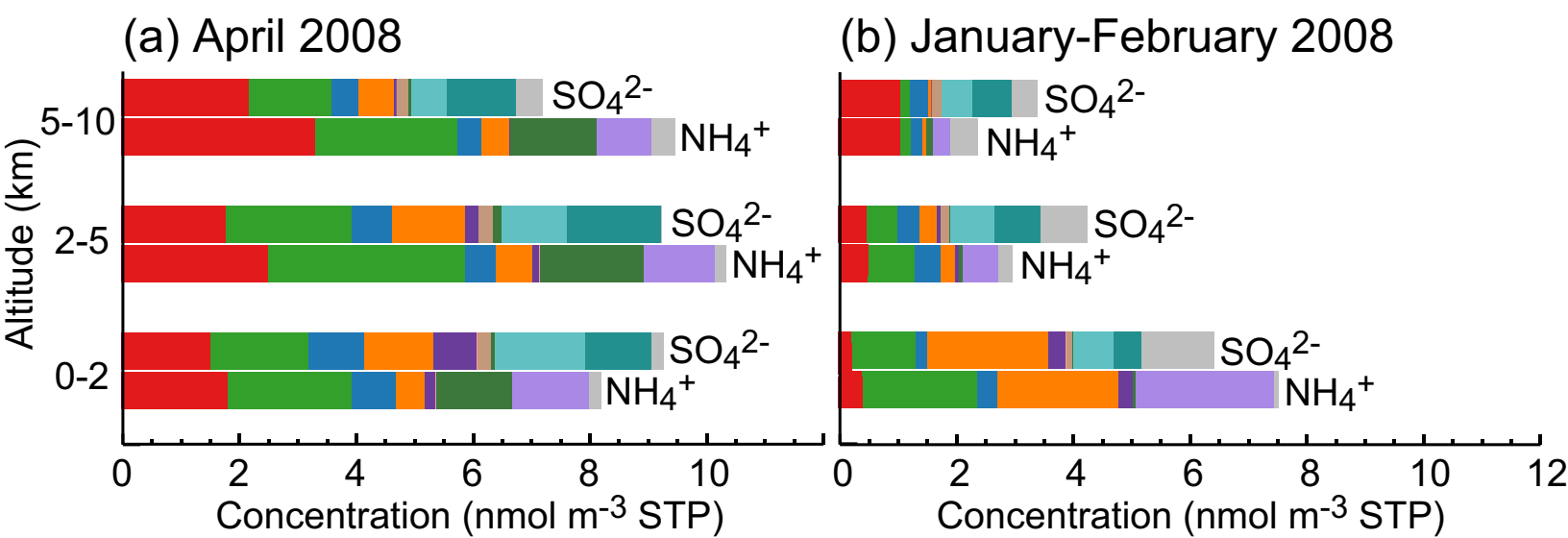


Figure8

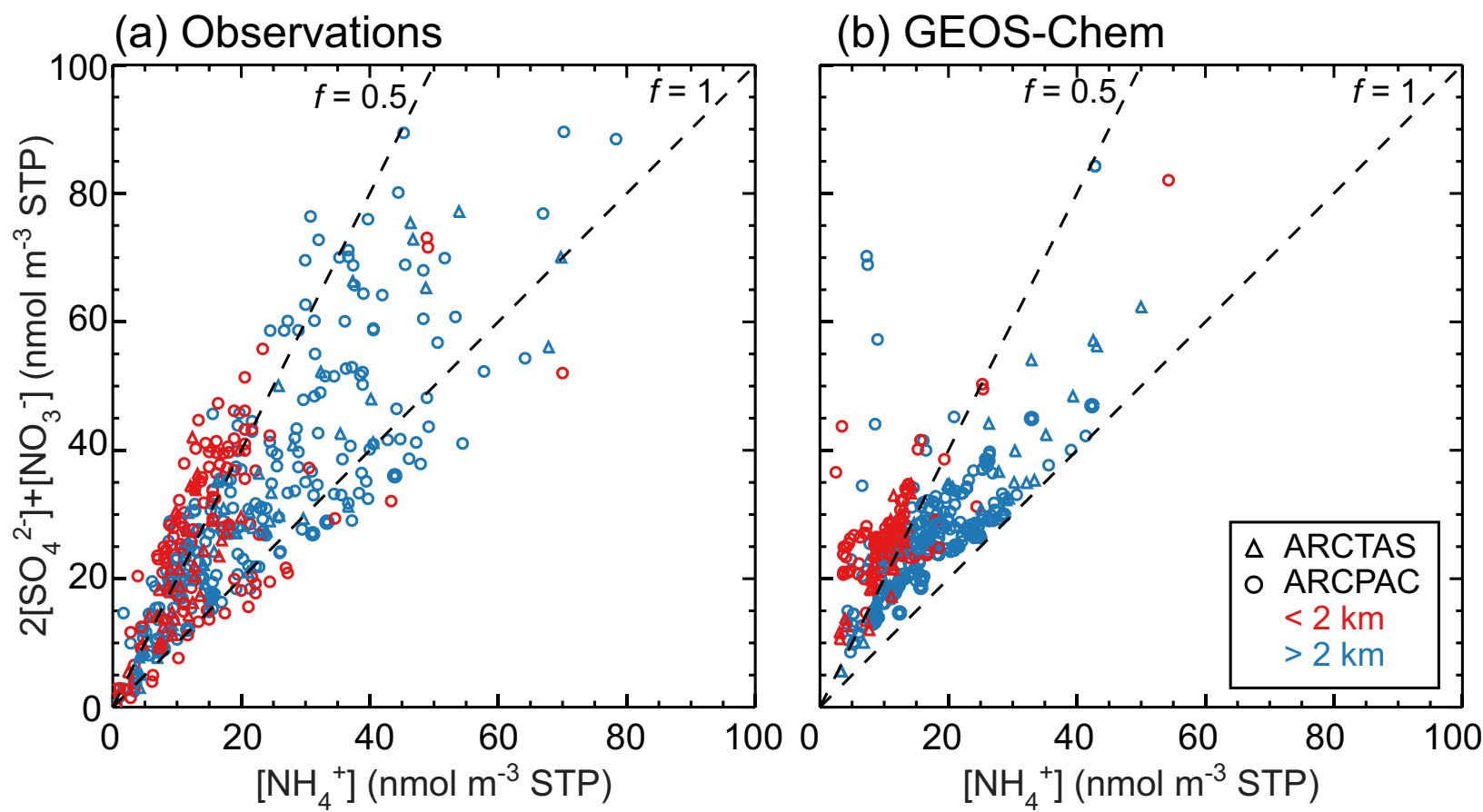


Figure9

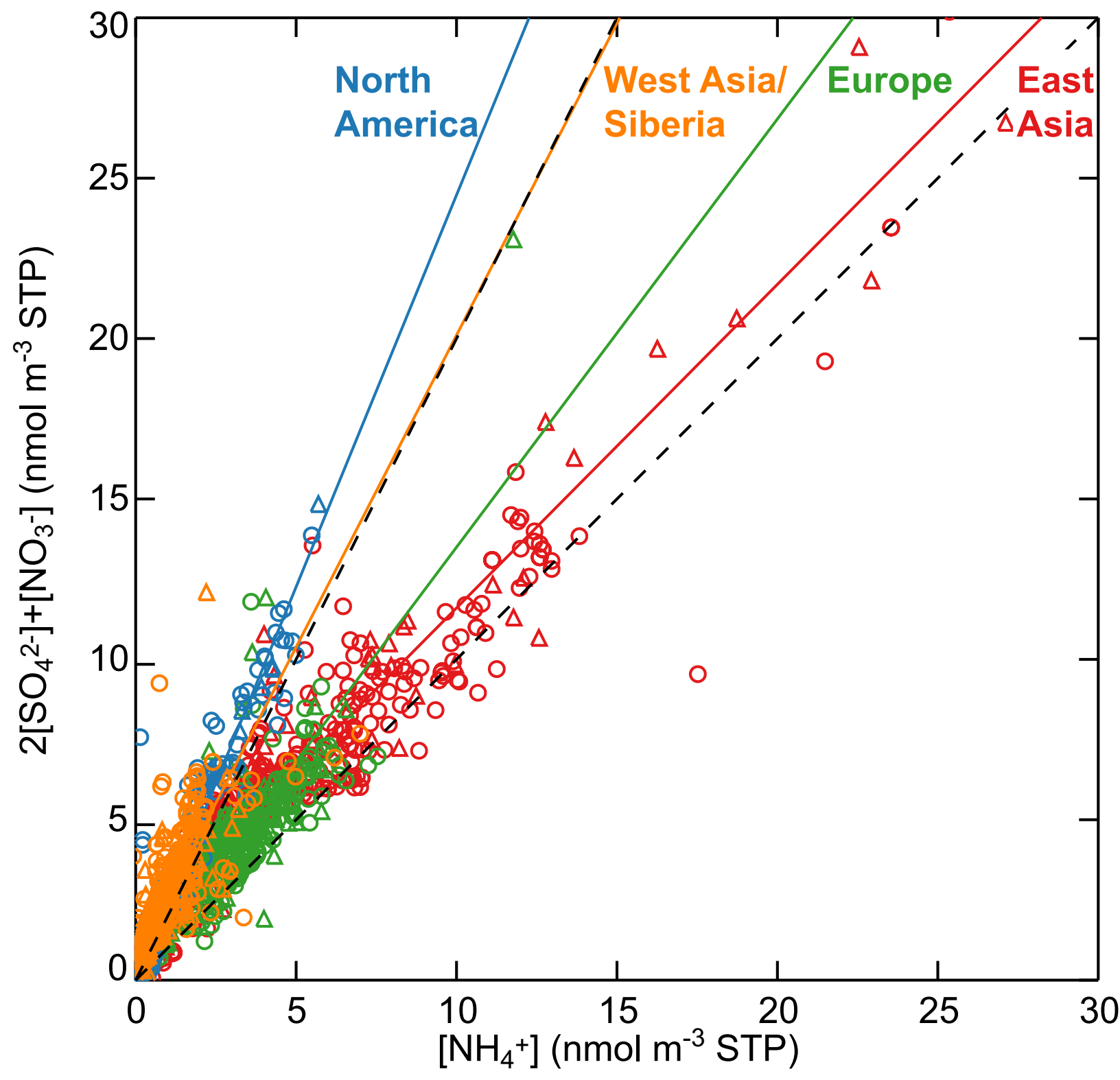


Figure10

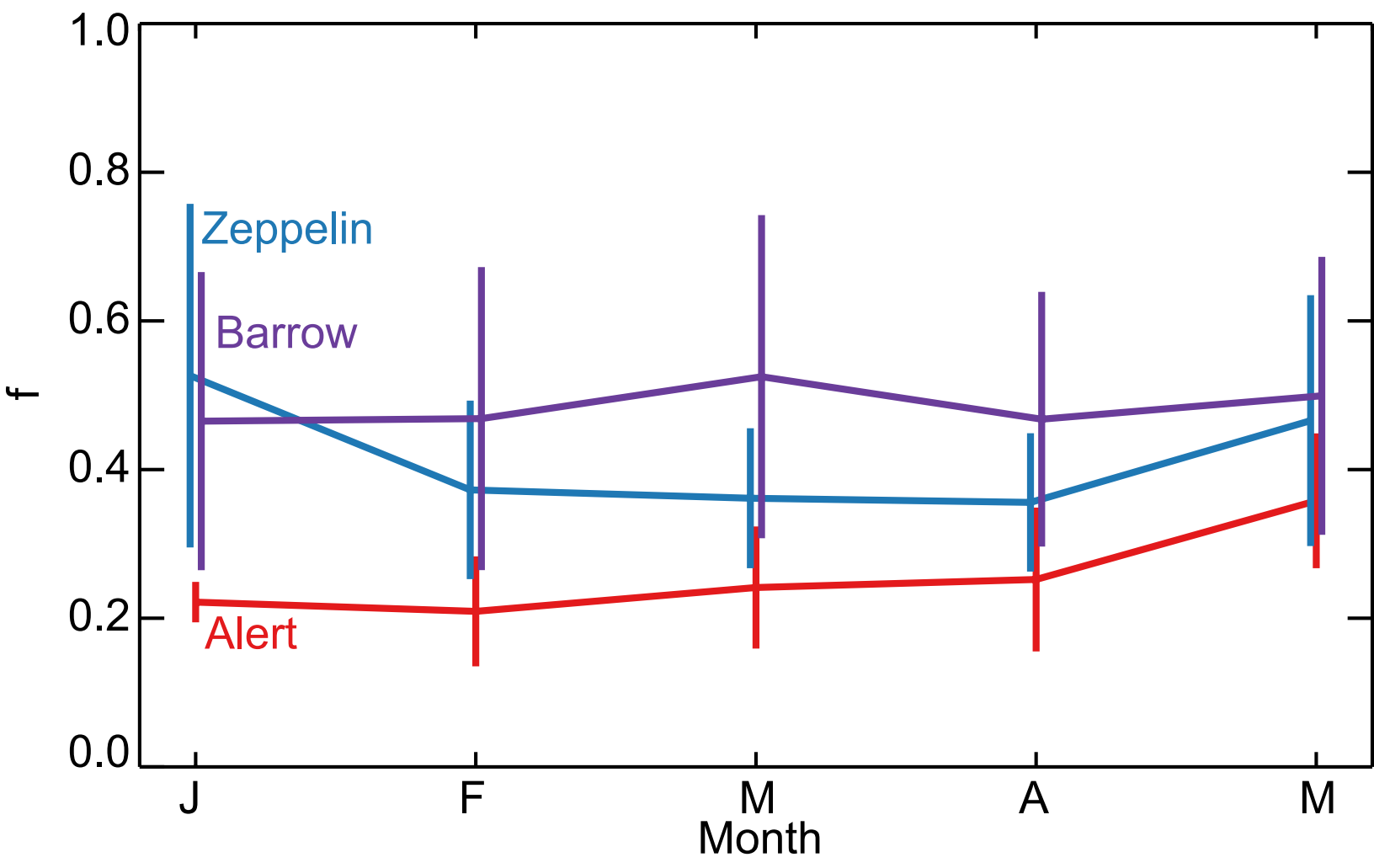
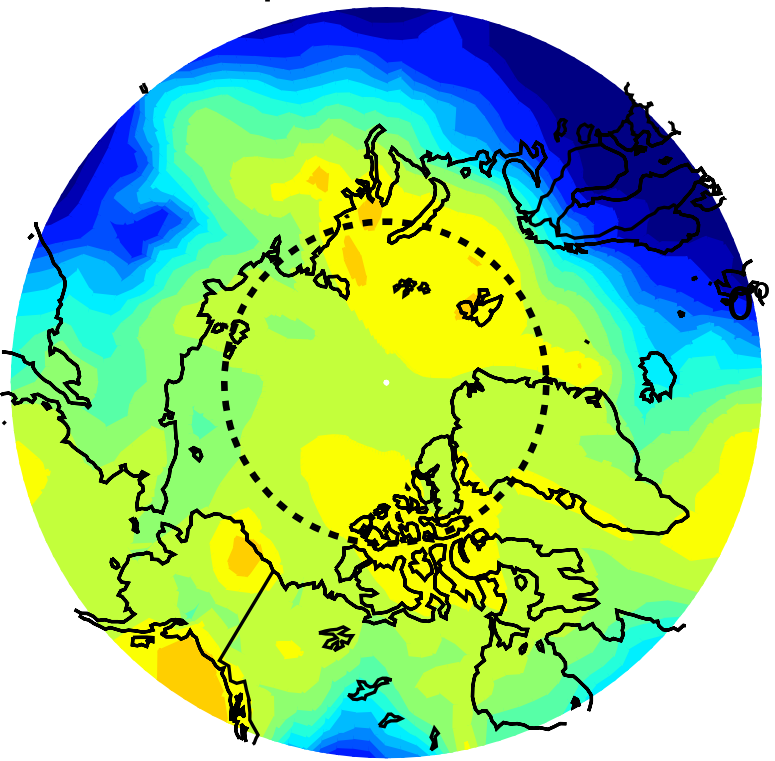
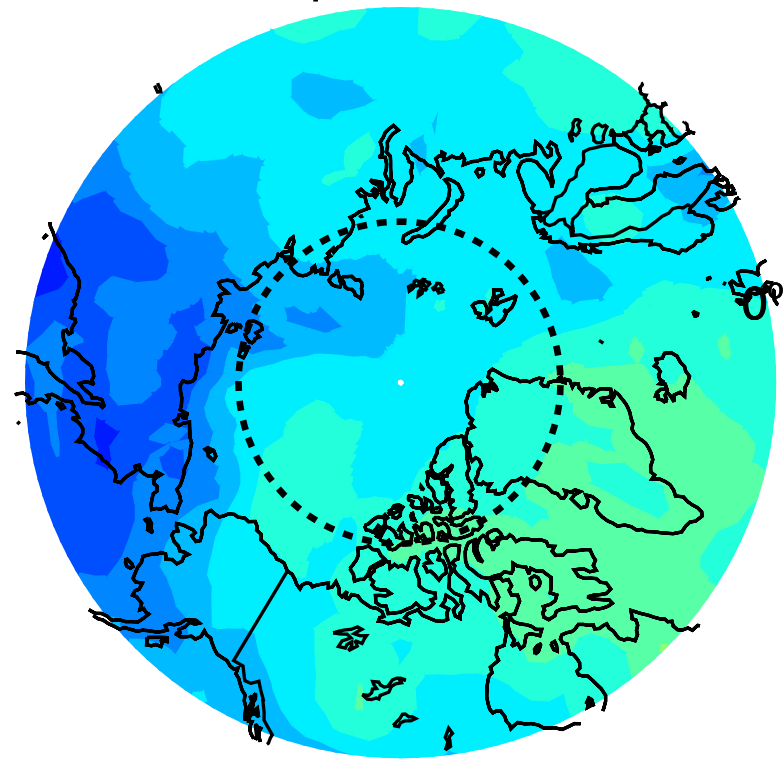


Figure11

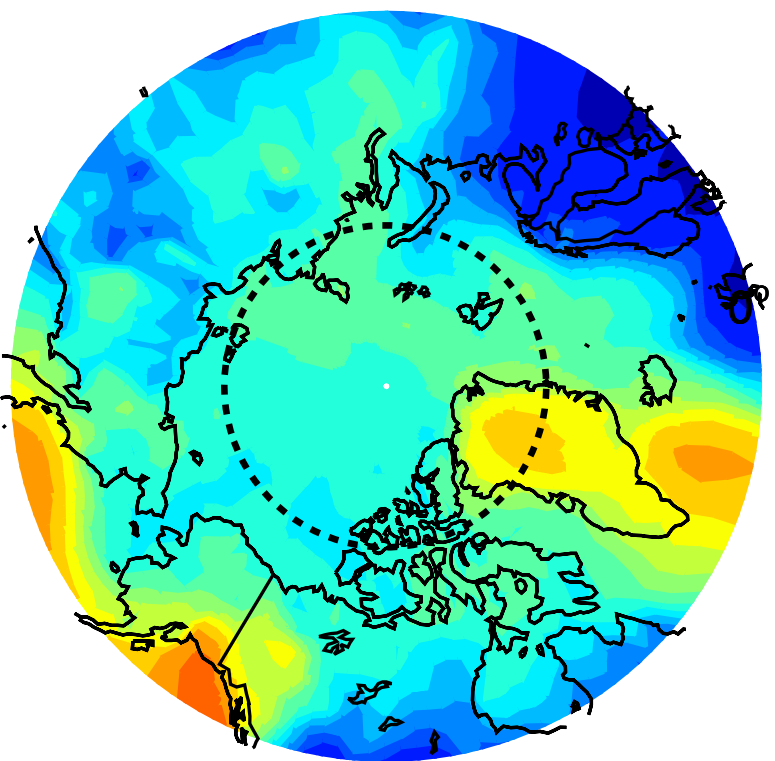
April: Surface



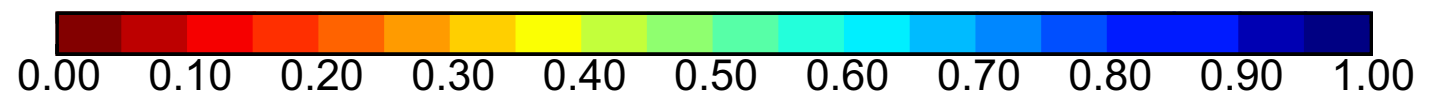
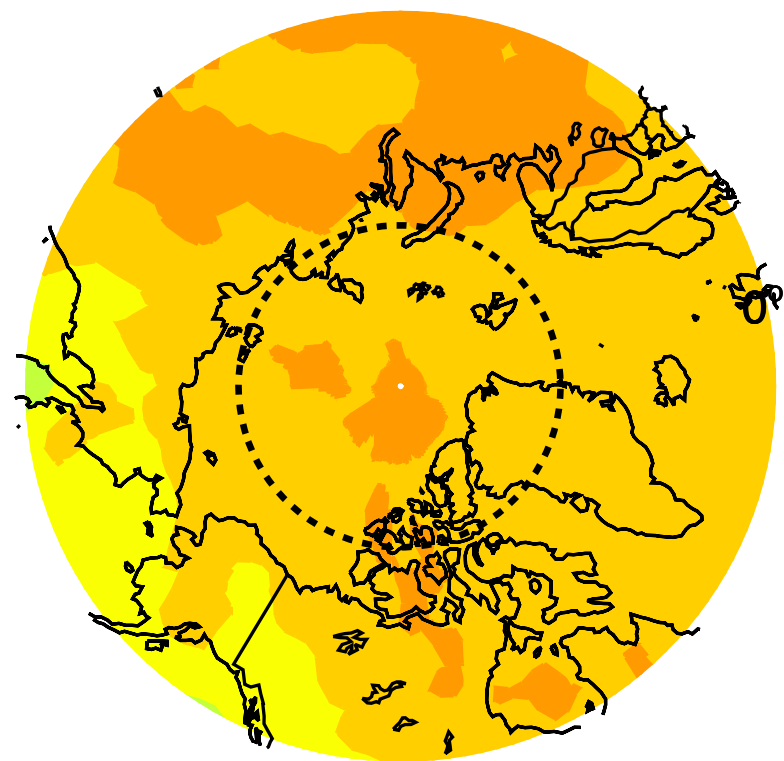
April: 5 km



Jan.-Feb.: Surface



Jan.-Feb.: 5 km



$$\frac{[\text{NH}_4^+]}{2[\text{SO}_4^{2-}] + [\text{NO}_3^-]}$$